

SPECT腦部影像品質定量分析

講師：楊邦宏 博士

臺北榮民總醫院核醫部

核醫腦部影像品質影響因子

- 藥物
 - 吸收特性、藥物標誌比活度、注射劑量
- 儀器
 - 儀器品管、準直儀、廠牌
- 病患
 - 檢查前準備事項、移動、病兆區域大小
- 收集影像條件
 - 收集的角度、時間，Zoom，繞360、矩陣大小、COR、距離
- 影像重建法
 - AC、SC、FBP、OSEM、Filter

SPECT BRAIN IMAGE PROTOCOL

Topic	#	Item	Parameter	Remark
Radiolotope for Phantom	1	99m-Tc	10-20mCi	
Image Device	2	Camera	SPECT SPECT/CT	
	3	Collimator	LEHR Fan Beam	
I. Image Acquisition				
SPECT Acq. Mode	1	Spatial Resolution	< 15mm (?)	
	2	Typical Radius of Rotation	12~15 cm	
	3	Photopeak (Energy Window)	140 keV \pm 10%	
	4	Matrix	128 x 128	
	5	Mode	Step-and-Shoot: Angle increments of 3°	
	6	Coverage of Head	360°	180° of each head of dual-head camera
	7	Scanning Duration	45 minutes	
	8	Total Counts	> 5 x 10 ⁶	
	9	Center of Rotation (COR)	< 1/10 of a pixel	Adjust for Fan Beam collimator
	10	Zoom	1.5	放大倍率影響計數
II. Image Post-Processing				
Projection Preview	1	Initial Evaluation	Linogram or Sinogram	For an initial determination of scan quality, patient motion, and artifacts
	2	Motion correction algorithms (?)		
Attenuation Correction	1	a. Radiation source	CT, Gd-153	
	2	b. First-order Chang's method	Linear Correction Coefficient = 0.12/cm for Tc-99m	
Image Reconstruction	1	a. Iterative reconstruction (IR)	Pixel Size 3.5~4.5 mm or 2.7~3.3 mm Slices: 1 pixel thick	
	2	b. Filtered BackProjection (FBP)	a. Butterworth (low-pass filtered) Slope of 6, cutoff of 0.55 b. Metz (band-pass filtered)	

觀念回顧

- Reliability: precision; reproducibility (信度)
- Accuracy : validity (效度)
- Bias: systematic or nonrandom difference between the true value of property; Prejudice.
- Error : measurement error
- Range : data distribution
- Standard deviation: range of variation surrounding the mean.

$$SD = \sqrt{\frac{\sum x^2}{M}}$$

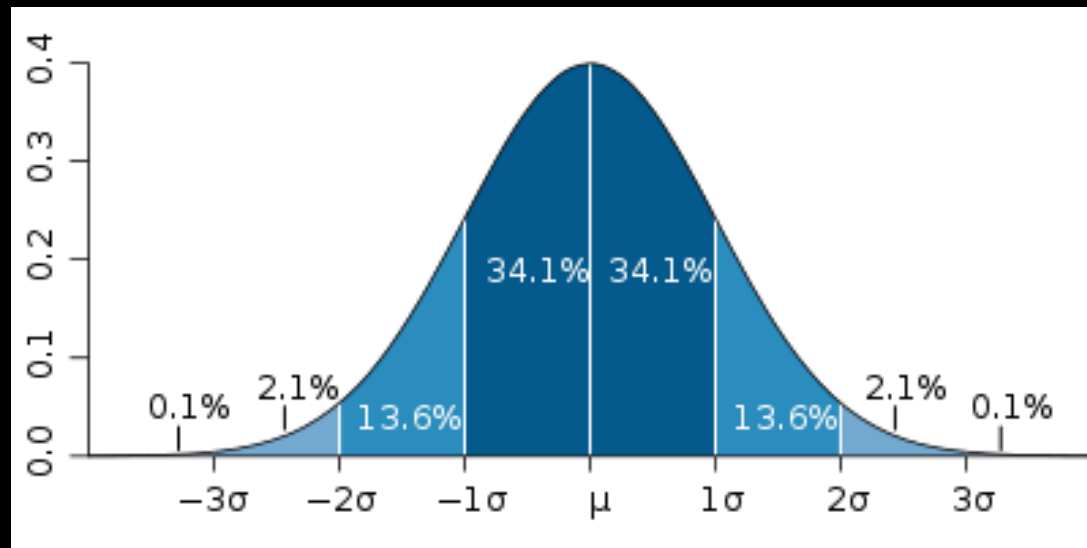
Example :

- With the values 7,3,6 and 4, the mean is 5.
What is the standard deviation ?

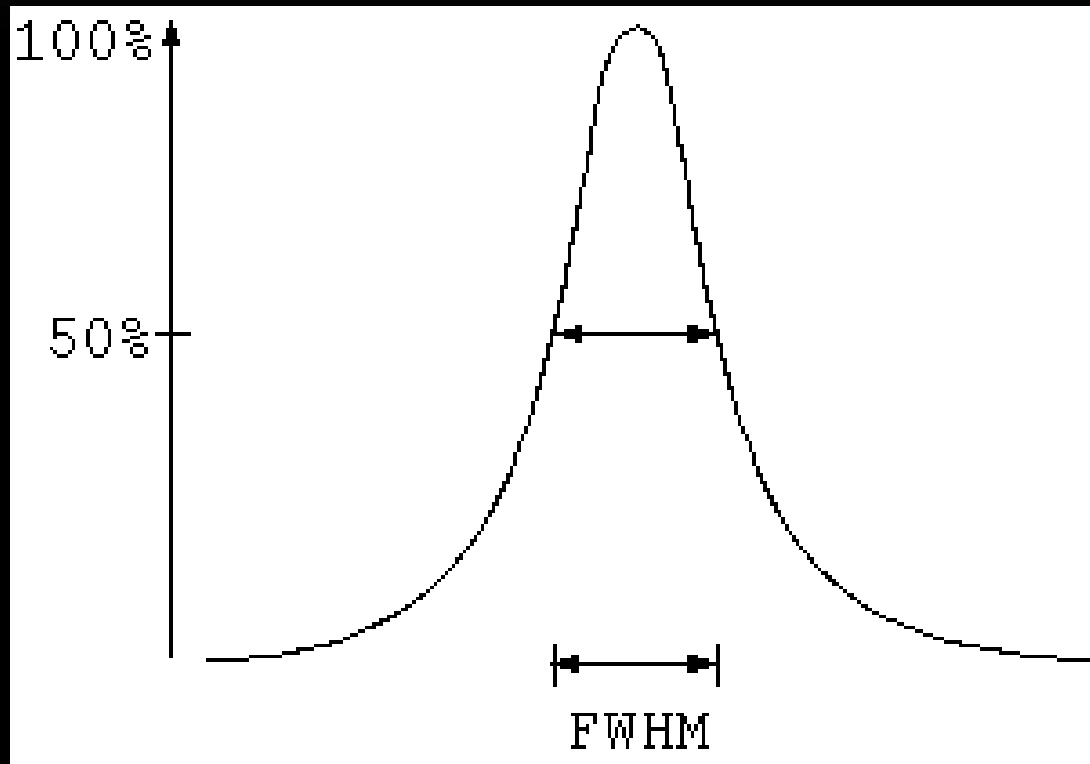
$$SD = \sqrt{\frac{\sum x^2}{M}} = \sqrt{\frac{(7-5)^2 + (3-5)^2 + (6-5)^2 + (4-5)^2}{5}}$$

$$SD = 1.41$$

- Variance : square of the SD
- Poisson distribution : random distribution in which the variance is equal to mean. In Poisson statistic in nuclear medicine, the SD can be estimated by taking the square root of mean.(ex. Mean=144, SD=12)
- Gaussian distribution : normal distribution or bell-shaped curve that is continuous w/ both tail extending to infinity.



Full width at half maximum(FWHM)



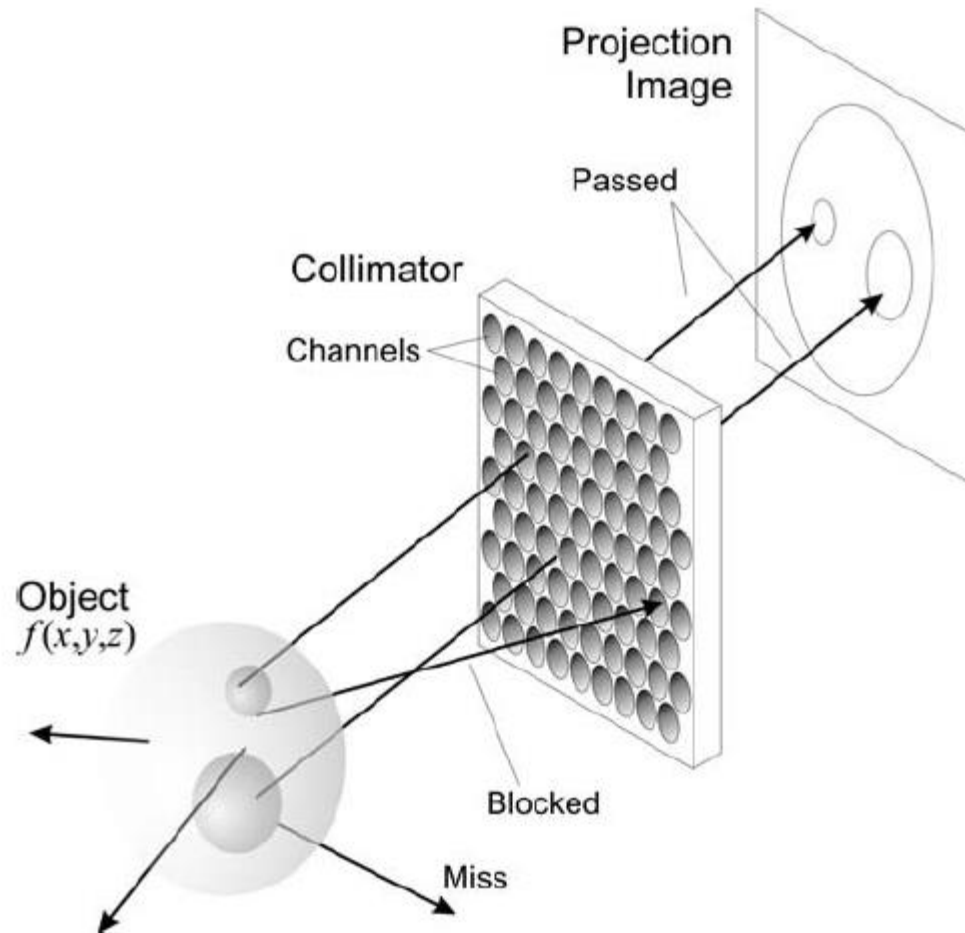


FIGURE 6 A collimator forms an image of the object by passing only rays traveling in a particular direction.

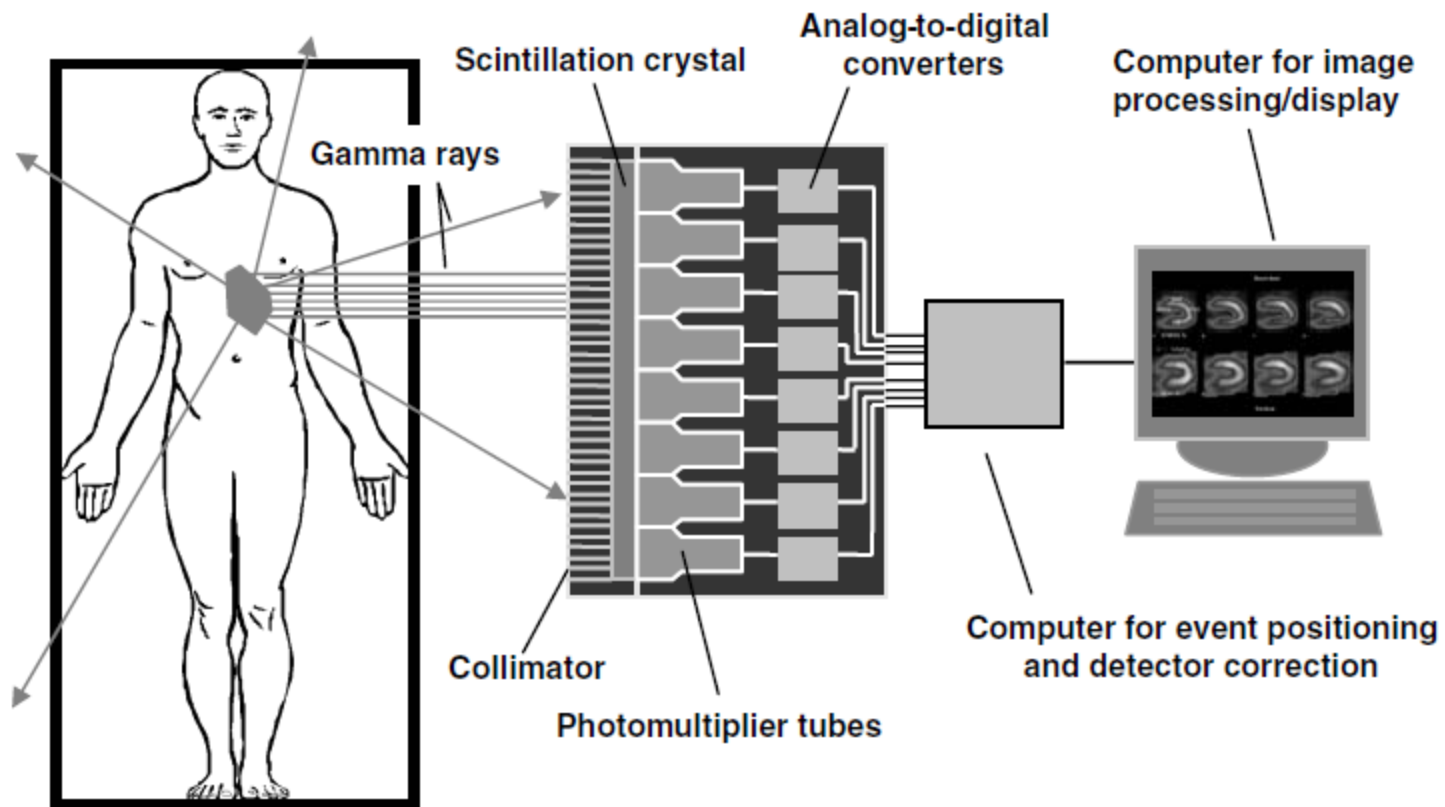


FIGURE 7 Schematic diagram of a conventional gamma camera used in SPECT. The collimator forms an image of the patient on the scintillation crystal, which converts gamma rays into light. The light is detected by photomultiplier tubes, the outputs of which are digitized and used to compute the spatial coordinates of each gamma-ray event (with respect to the camera face). A computer is used to process, store, and display the images.

PROJECTIONS

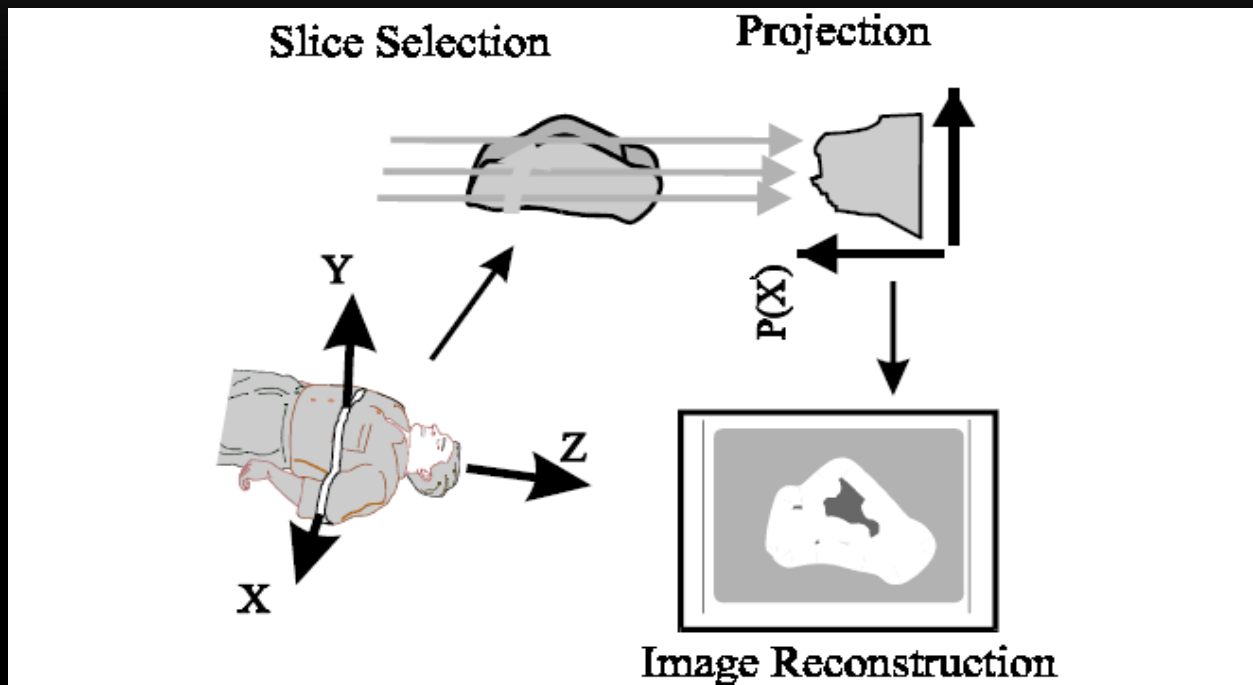


Figure 1.1 The tomographic process generally consists of three steps. First a single slice is selected. Next a complete set of projections of that slice is obtained. Finally the set of projections are recombined, using a mathematical recipe, to form a reconstructed image of the slice.

Basics of Imaging Theory and Statistics

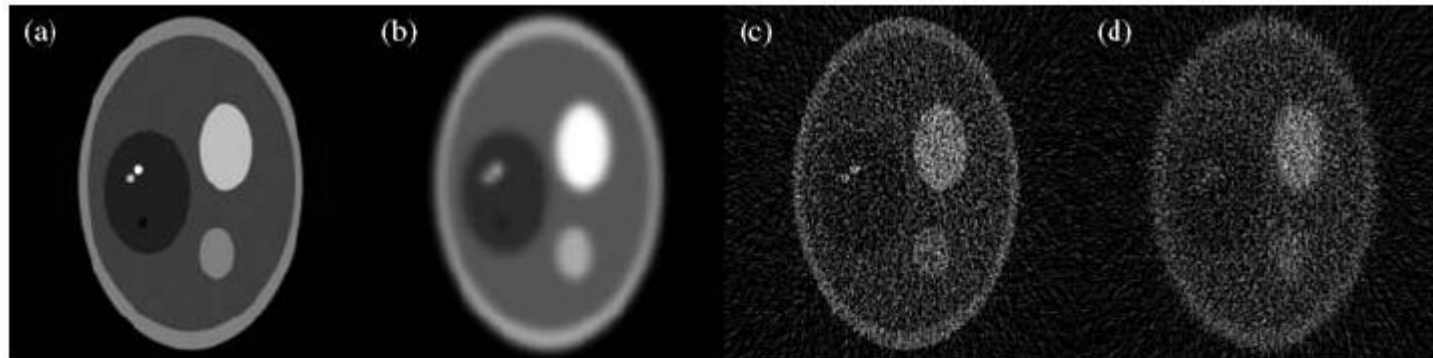


FIGURE 1 Effects of blur and noise on image quality. Images shown are (a) an ideal image of a mathematical phantom, (b) the same image degraded by blur, (c) the same image degraded by noise, and (d) the same image degraded by both blur and noise. As shown, image blur leads to loss of image contrast and definitions. Image noise results in intensity fluctuations, also making small low-contrast structures difficult to resolve.

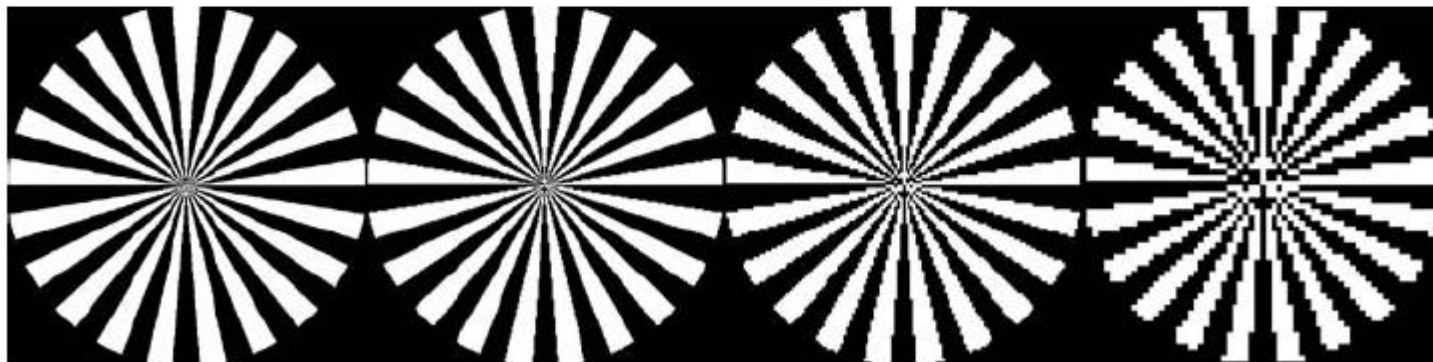


FIGURE 2 Illustration of sampling effects. From left to right, the images shown are the same spatial pattern sampled by 512×512 , 256×256 , 128×128 , and 64×64 rectangular grids. Aliasing errors can be observed at the centers of these images. These errors become more pronounced as the grid size decreases.

MATRIX SIZE

- SPECT systems, FOV (with zoom =1) is precalibrated by the manufacturer, the size of a pixel, D, in millimeters, may be calculated:

$$D = \text{FOV}/(Z \times n), \quad \text{Eq. 1}$$

where:

FOV (mm) = the widest dimension of the computer image matrix

Z = zoom factor (e.g., 1.5, 2.0, etc.) during acquisition

n = number of pixels (e.g., 64 or 128).

128x128 image will only have **1/4** the counts per pixel as the corresponding 64X64 image.

Some basic properties of the frequency domain

- The **low frequency** correspond to the **slowly varying** components of an image
- The **higher frequency** correspond to the **faster gray level changes** in an image

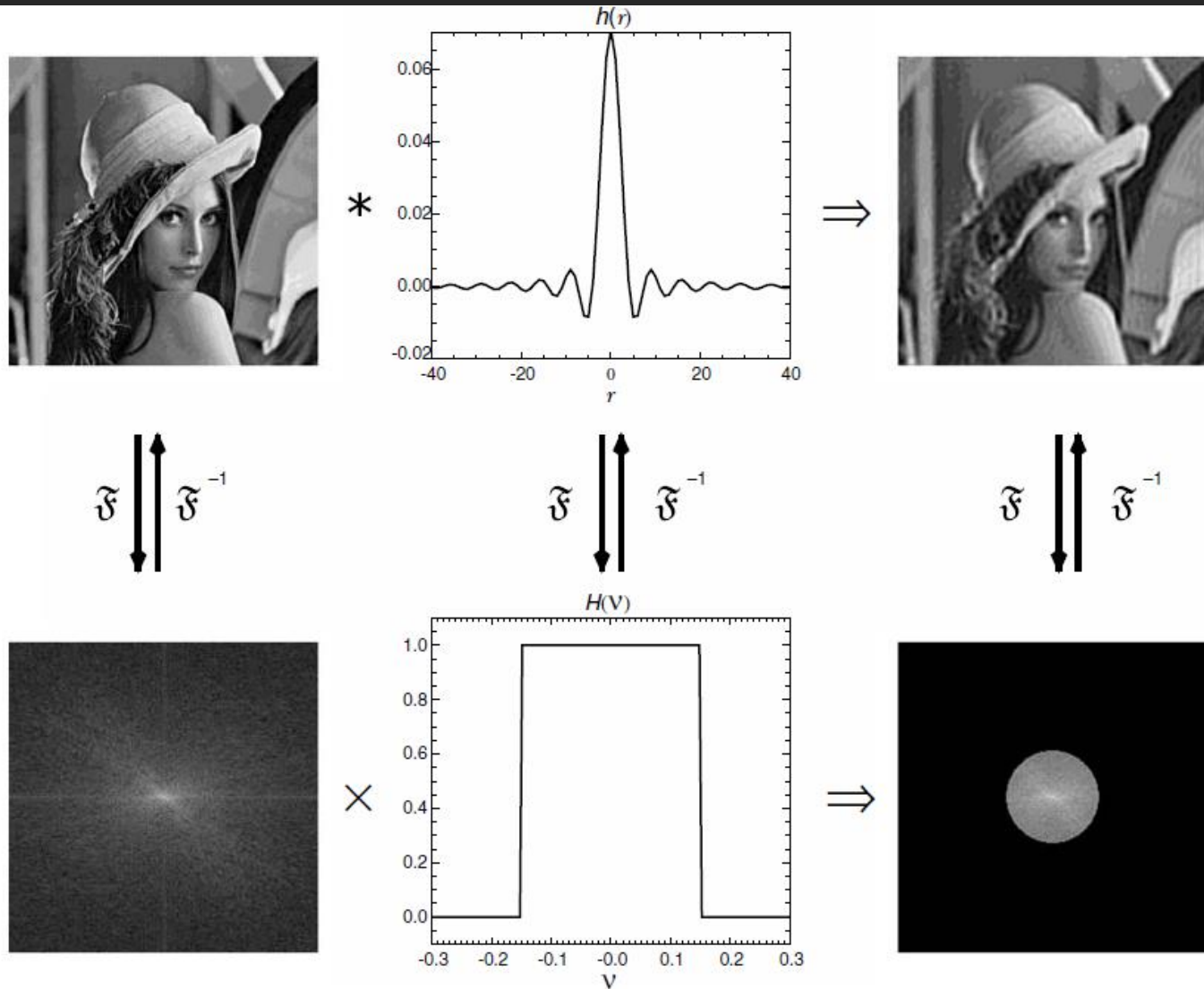


FIGURE 3 Ideal lowpass filtering of an image. Figures in the top and bottom rows demonstrate the filtering operation in the spatial and frequency domains, respectively. The left column shows the input image and the magnitude of its Fourier transform. The middle column are the circular symmetric PSF and its transfer function, where $v = \sqrt{v_x^2 + v_y^2}$ and $r = \sqrt{x^2 + y^2}$. Images in the right column are the output image and the magnitude of its Fourier transform.

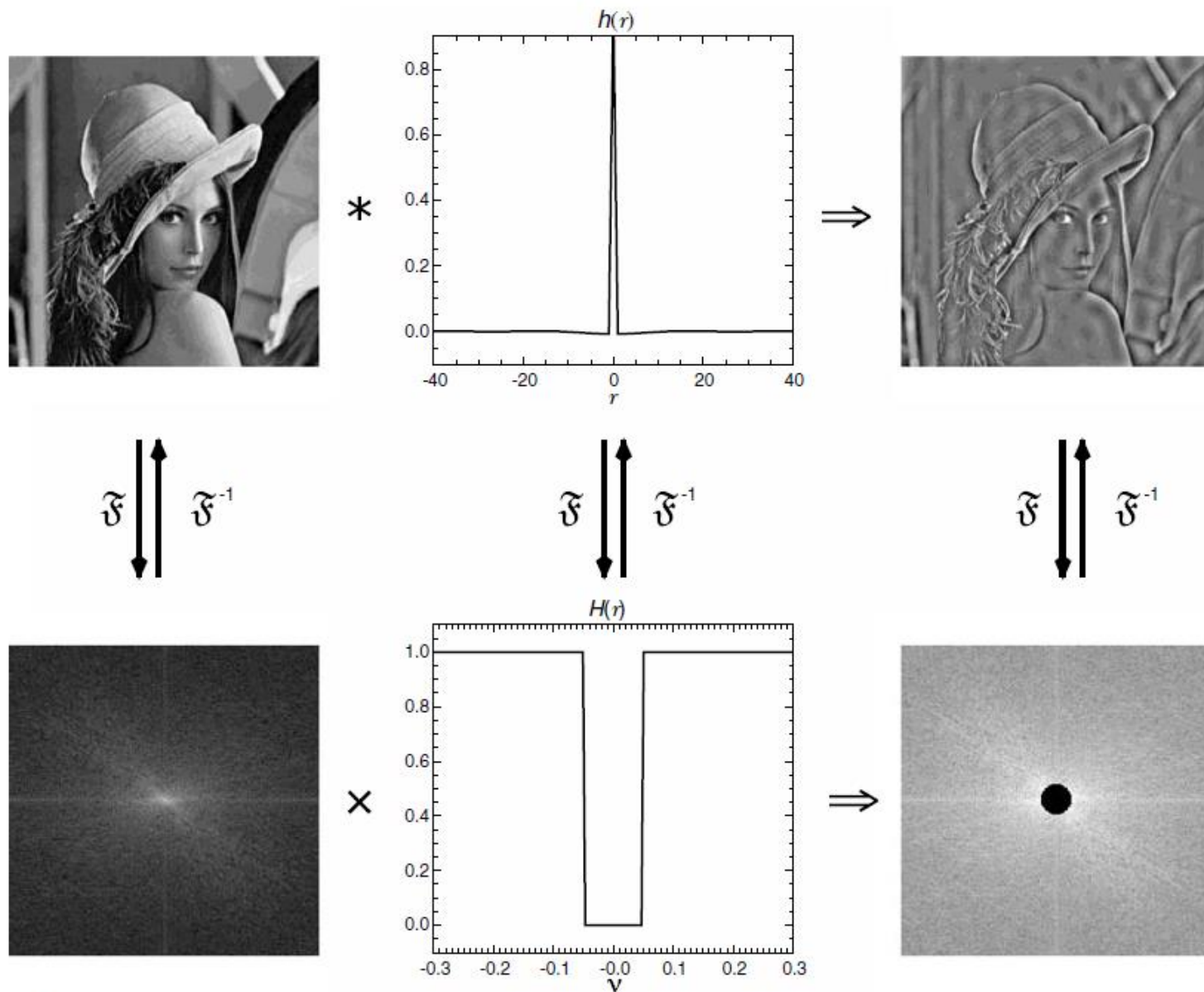
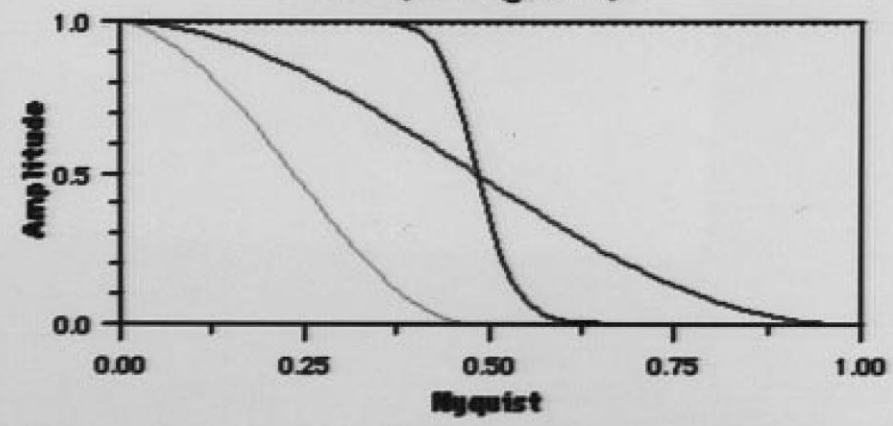


FIGURE 4 Ideal highpass filtering of an image. Figures in the top and bottom rows demonstrate the filtering operation in the spatial and frequency domains, respectively. The left column shows the input image and the magnitude of its Fourier transform. The middle column shows the circular symmetric PSF and its transfer function, where $v = \sqrt{v_x^2 + v_y^2}$ and $r = \sqrt{x^2 + y^2}$. Images in the right column are the output image and the magnitude of its Fourier transform.

Speed

Frequency Graph



Curve Recon Filter

Cutoff:
 Alpha:
 Order:

Resultant Transverses

GenHamm: 1.0, 5 GenHamm: 3, 5 ButterV: .5, 10 BandLimRamp: 1.0

Filter 1

Filter 2

Filter 3

Filter 4

COUNTS FACTOR

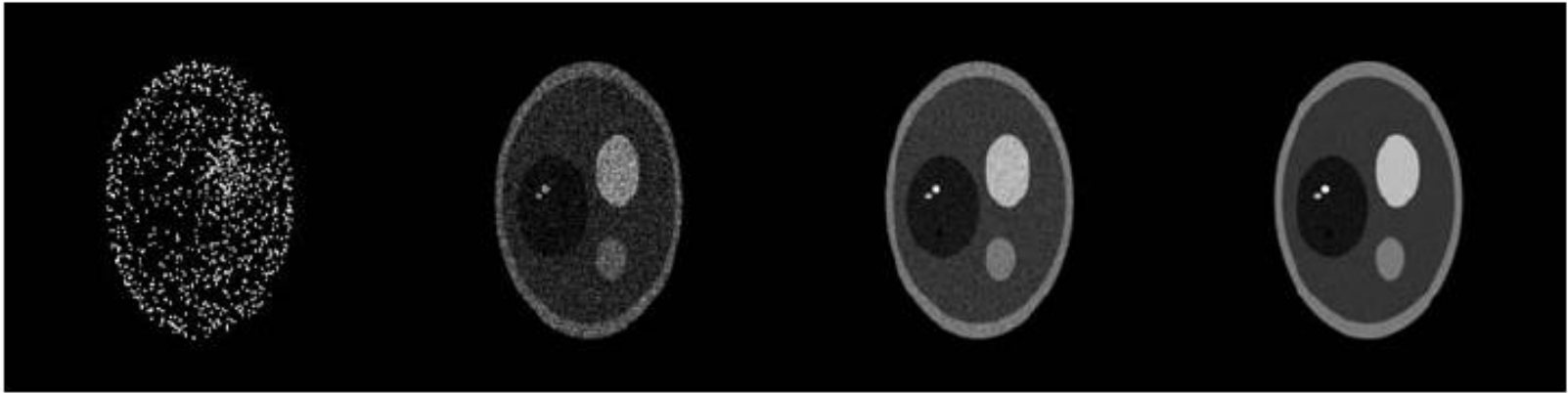
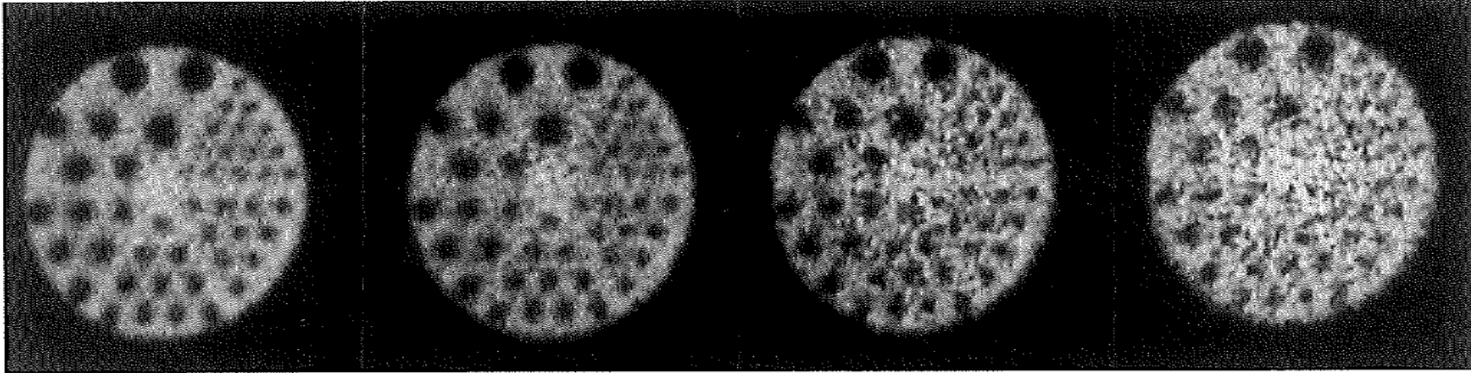


FIGURE 8 Example noisy images of a mathematical phantom, corrupted by Poisson noise. From left to right, the images contain 10^3 , 10^5 , 10^6 , and 10^{11} total photon counts.

BENCHMARK COLD RODS



11 Million

5.5 Million

2 Million

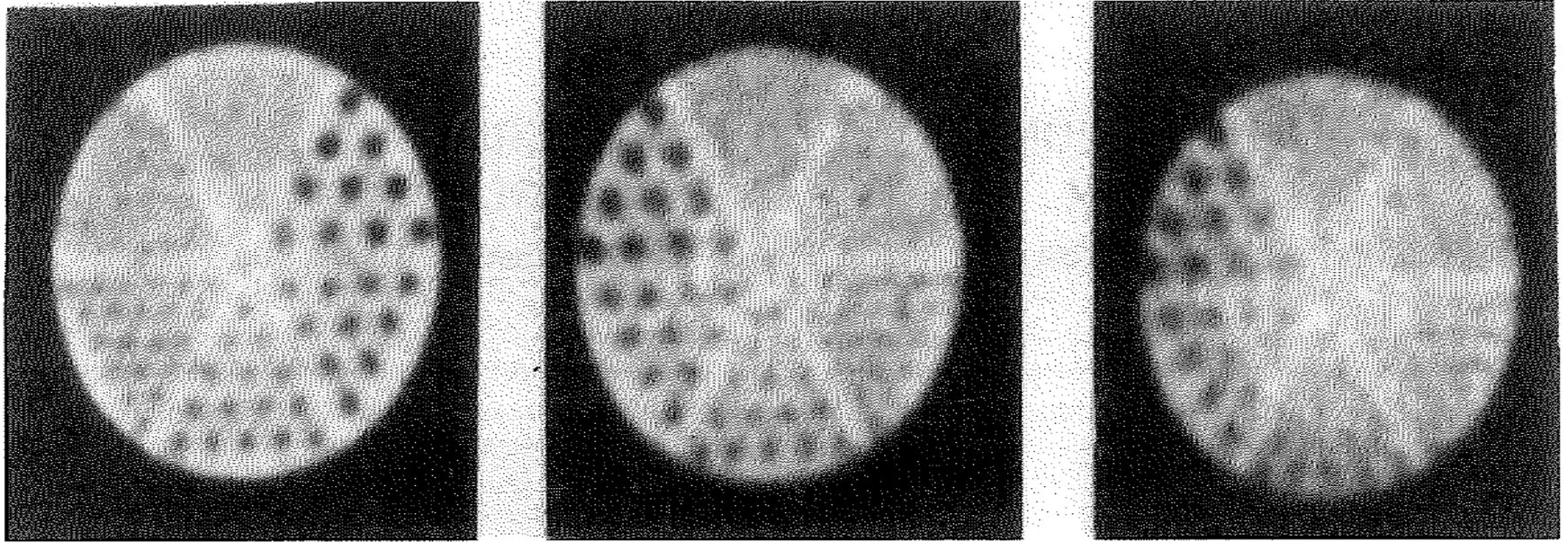
1. Million

EFFECT OF TOTAL COUNTS IN SLICE

Collimators	LEHS	LEAP	LEHR	LEUHR	LEFB	ME	HE	UHE
	Low Energy High Sensitivity	Low Energy All Purpose	Low Energy High Resolution	Low Energy Ultrahigh Resolution	Low Energy Fanbeam	Medium Energy	High Energy	Ultrahigh Energy
Isotope	^{99m} Tc	^{99m} Tc	^{99m} Tc	^{99m} Tc	^{99m} Tc	⁶⁷ Ga	¹³¹ I	¹⁸ F
Hole Shape	Hex	Hex	Hex	Hex	Hex	Hex	Hex	Hex
Number of Holes (x 1,000)	28	90	148	146	64	14	8	4
Hole Length (mm)	24.05	24.1	24.05	35.8	35	40.64	50.8	50.5
Septal Thickness (mm)	0.36	0.20	0.16	0.13	0.16	1.14	2	3.4
Hole Diameter (mm across the flats)	2.54	1.45	1.11	1.16	1.53	2.94	3.4	2.5
Sensitivity @ 10 cm (cpm/μCi) ¹	1020	330	202	100	280	310	135	185
Geometric Resolution @ 10 cm (mm)	14.6	8.3	6.4	4.6	6.3	10.8	12.6	10.6
System Resolution @ 10 cm (mm) ¹	15.6	9.4	7.4	6.0	7.3	12.5	14.5	19.0
Septal Penetration (%)	1.5	1.9	1.5	0.8	1	1.2	3.5	3.4
Focal Length @ Exit Surface (mm)	n.a.	n.a.	n.a.	n.a.	445	n.a.	n.a.	n.a.
Weight in lb.	42	49	45	56	67	136	245	260
Weight in kg	18.9	22.1	20.4	25.2	30.5	61.8	111.1	117.0

1. Values measured in accordance with NEMA Standards Publication NU-1 2001 using 3/8" crystal.

DELUXE COLD RODS



**Ultra-High Resolution
Collimator**

Rel. Sensitivity: 0.24

**High Resolution
Collimator**

Rel. Sensitivity: 0.64

**Low Energy, All-
Purpose Collimator**

Rel. Sensitivity: 1.0

EFFECT OF COLLIMATION

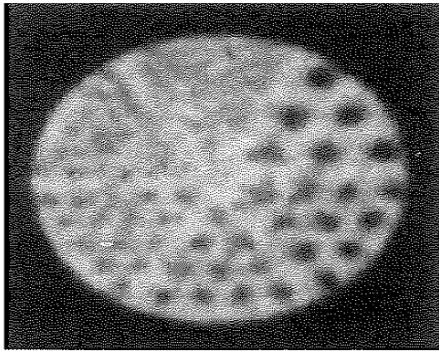
STANDARD COLD RODS

HIGH RESOLUTION COLLIMATOR

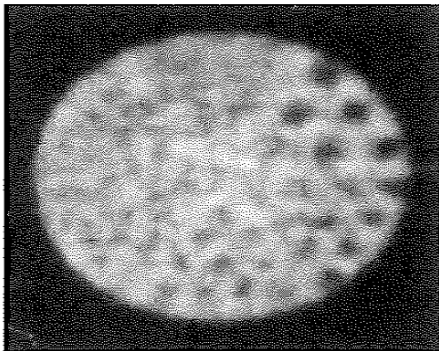
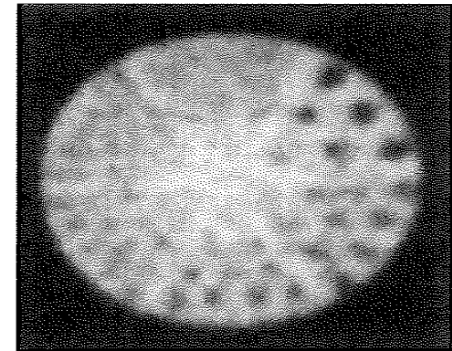
Approximately 8 million cnts

LOW ENERGY, ALL PURPOSE COLLIMATOR.

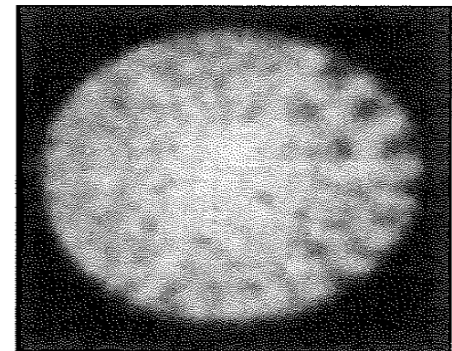
Approximately 10 million cnts.



ROR
14cm

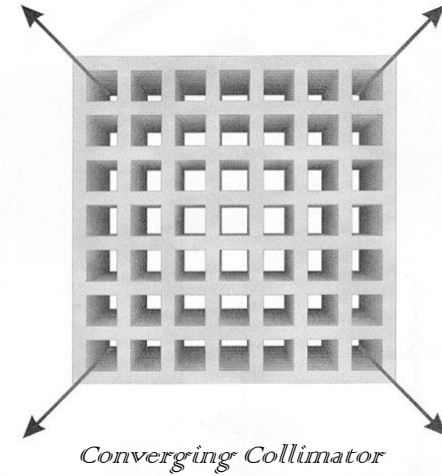
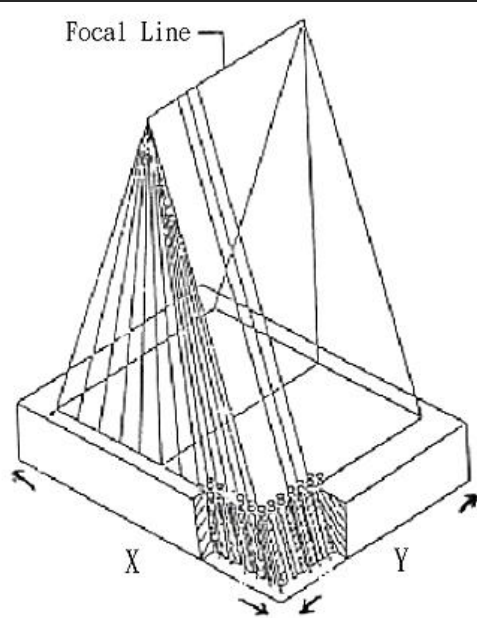


ROR
22cm

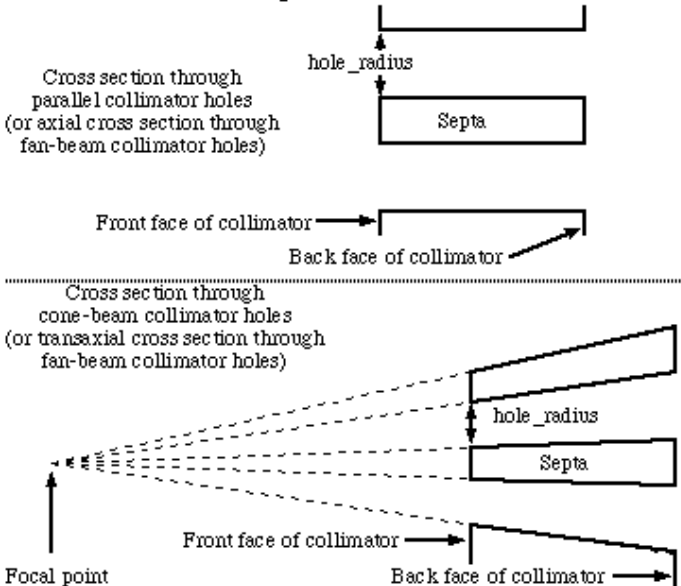


EFFECT OF RADIUS-OF-ROTATION

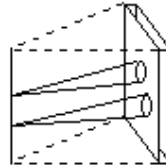
扇形式多孔準直儀 (*Fan Beam Collimators*)



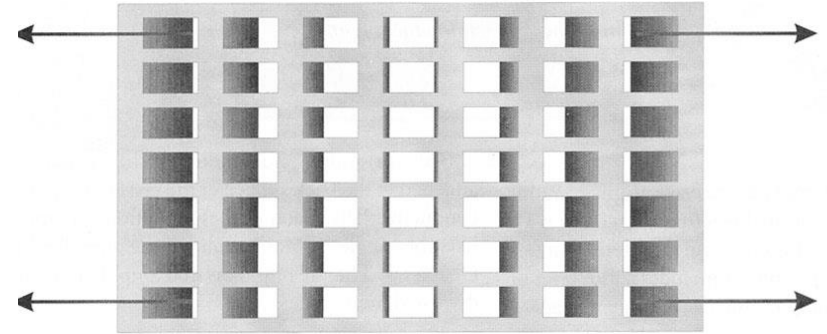
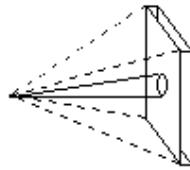
Cross sections through collimator holes



A fan-beam hole focuses to a point on the focal line that is at the same transaxial level as the hole



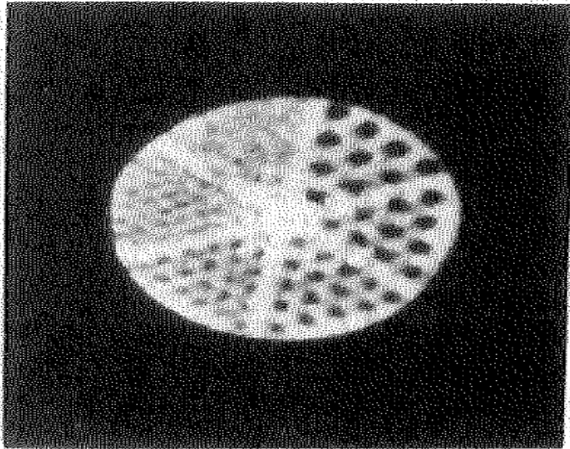
In cone beam, all holes focus on a single point.



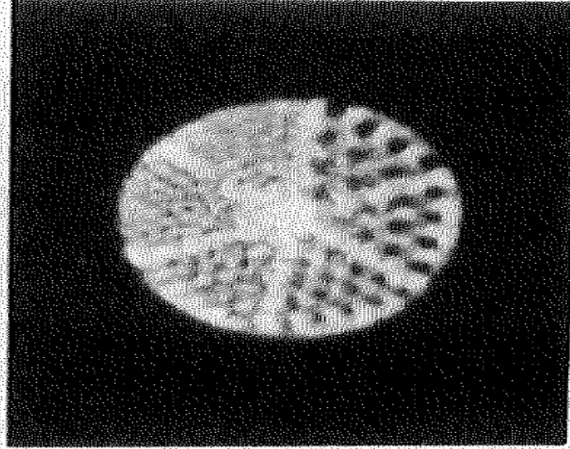
Fan Beam Collimator

RF

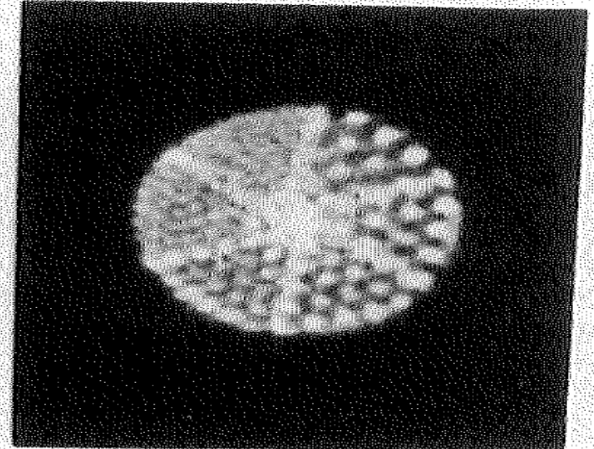
DELUXE COLD RODS



ALIGNED



MISALIGNED
(3.2mm)



MISALIGNED
(6.4mm)

EFFECT OF CENTER-OF-ROTATION CALIBRATION

Signal to noise ratio (SNR)

- Signal-to-noise ratio is defined as the power ratio between a signal (meaningful information) and the background noise (unwanted signal).

$$\text{SNR} = \frac{P_{\text{signal}}}{P_{\text{noise}}}$$

Modulation Transfer Function

- Good **low frequency** response is needed to outline the coarse details of the image and is important for the presentation and detection of relatively large but low contrast lesion.
- Good **high frequency** response is necessary to portray fine details and sharp edges.
- A typical nuclear medicine image system transfers **lower spatial frequencies image.**

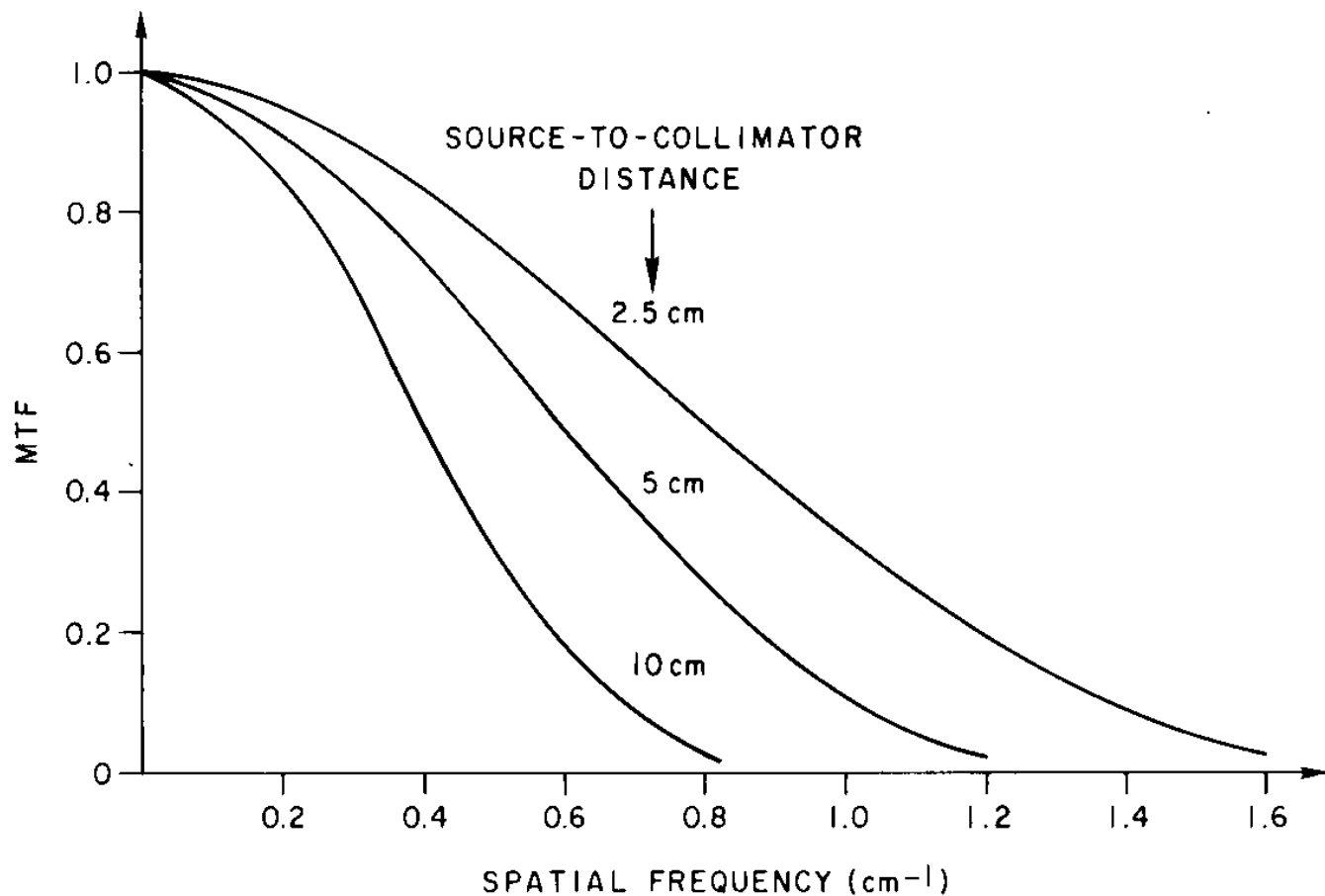


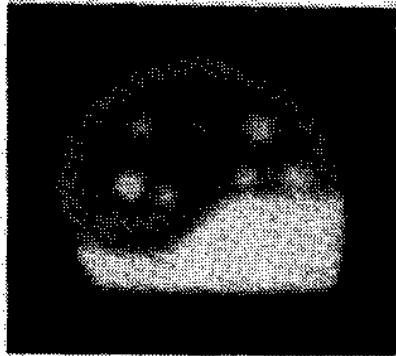
Fig. 18-6. MTF curves for a typical parallel-hole collimator for different source-to-collimator distances. [Data from ref. 1: Ehrhardt JC, Oberly LW, Cuevas JM: Imaging ability of collimators in nuclear medicine. Rockville, Md., U.S. Dept. H.E.W., Publ. No. (FDA)79-8077, p. 39, 1978. With permission.]

Contrast

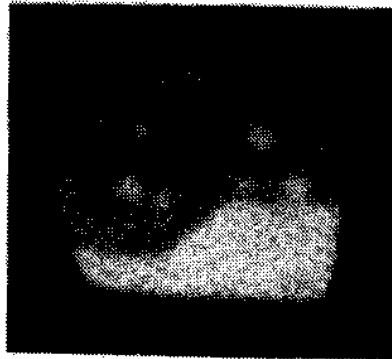
- Background count rates can reduce the image contrast substantially.
- **Scattered** radiation and septal penetration have the same effect of adding background to the image.
- Pulse height analyzer (narrow the window) could be used for the scatter rejection but there is a trade-off (**decrease counts and increase noise**)
- Decreased contrast (background, scatter or septal penetration) results in poorer visibility of both large low contrast objects as well as fine details (all structures) in the image.
- **Scatters** add long tails to the spread function, suppress the low frequencies and shift the limiting high frequency in MTF.

Contrast

- Image contrast refers to the differences in **density** (or intensity) in parts of the image.
- There are a number of factors that could affect the contrast such as the **radiopharmaceuticals** (high lesion-to-background uptake desirable)
- **Film contrast** (transparency has better contrast than Polaroid film) enhance both desire image **contrast and noise**.



20 % WINDOW
IN AIR



20 % WINDOW



50 % WINDOW

IN SCATTERING MEDIUM

Fig. 18-10. Effect of scatter and pulse-height analysis on contrast of brain phantom images.

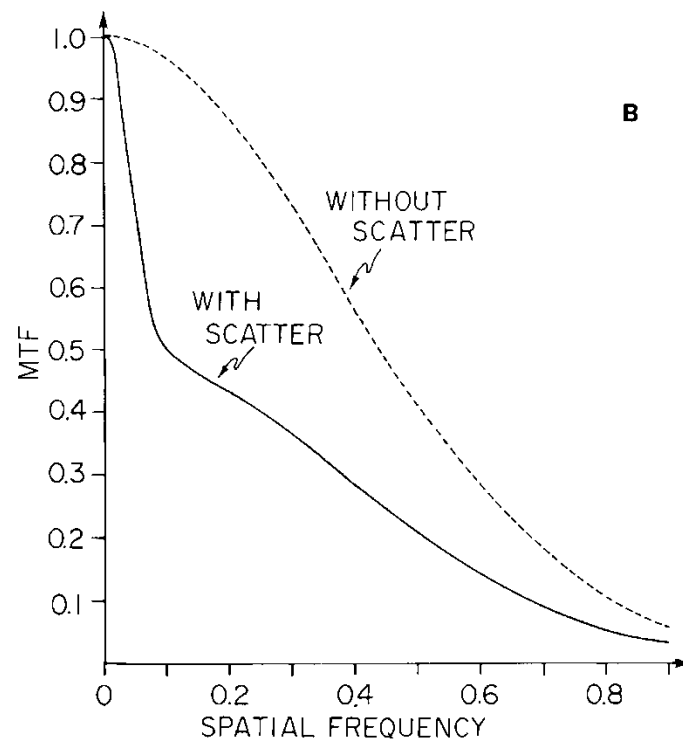
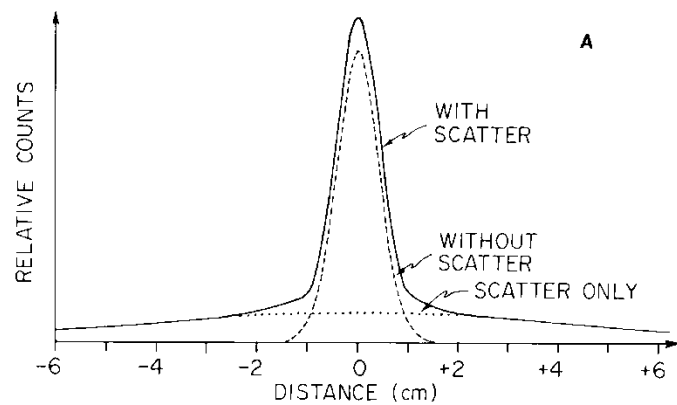


Fig. 18-11. Demonstration of effects of scatter and/or septal penetration on line spread function (A) and MTF (B) of an imaging system. The long "tails" on the LSF have the effect of suppressing the MTF curve at both low and high spatial frequencies.

Noise

- Image noise may be either **random** or **structured**
 - **Structured noise** refers to non-random variation in counting rate superimposed on and interfering with the perception of the structures of interest
 - Structured noise may arise from the radionuclide distribution itself or caused by **system artefacts**.
 - **Random noise** is caused by **statistical variation** of count rate and is very important factor in nuclear medicine.
-

Random Noise

- Random noise is related to the information density
 - Information density is defined as the counts per unit area recorded
 - Information density can be increased by increase **count rate or imaging time**
 - Information density affects the minimum **detectable size** and **contrast of lesions**.
-

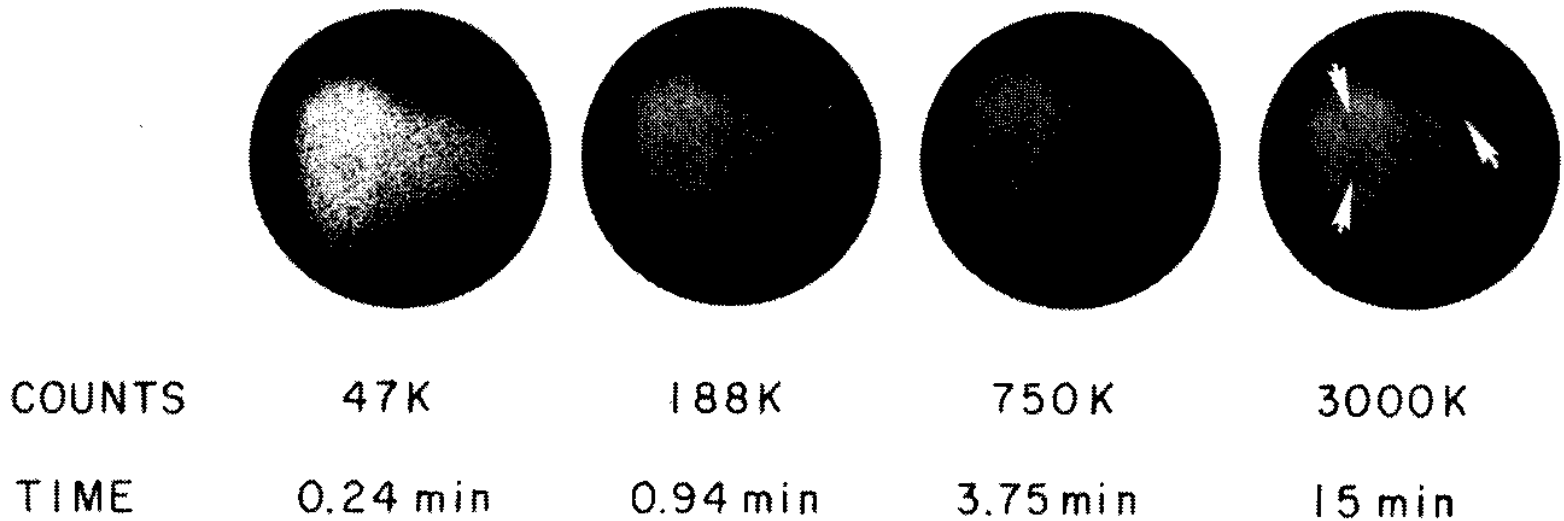


Fig. 18-13. Example of effects of information density on perceptibility of low-contrast lesions in a liver phantom. There are two lesions in the right lobe. One very small lesion in the left lobe is seen only with the highest information density.

Noise vs Lesion Contrast

- Noise contrast is the **percentage standard deviation** of counts recorded in an area
- A **3-5 times** the noise contrast is required for a lesion to be detectable
- Lesion contrast requirement increases as lesion size decrease
- Random noise may be the detection limiting factor for **small, low contrast lesions.**

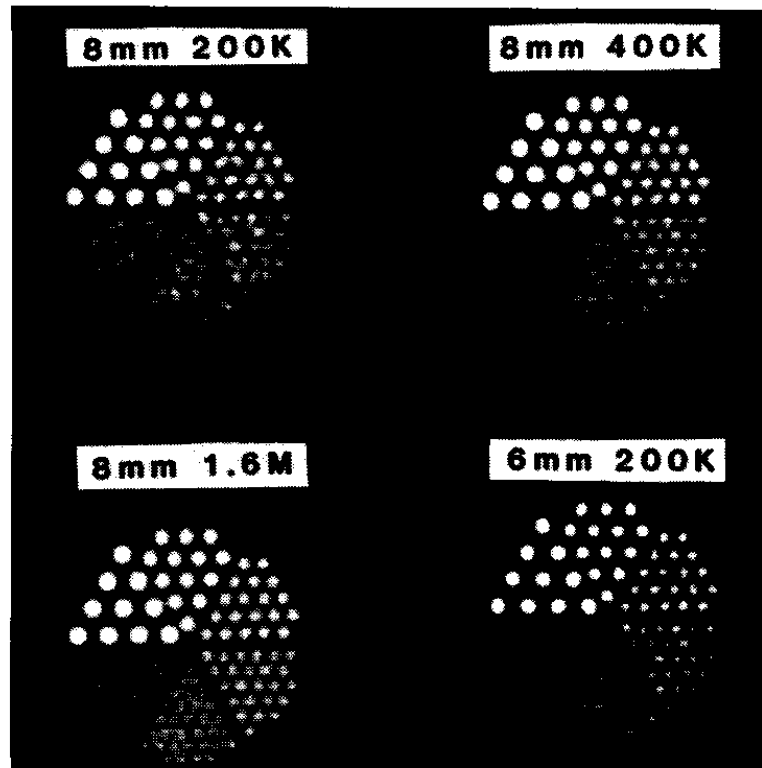
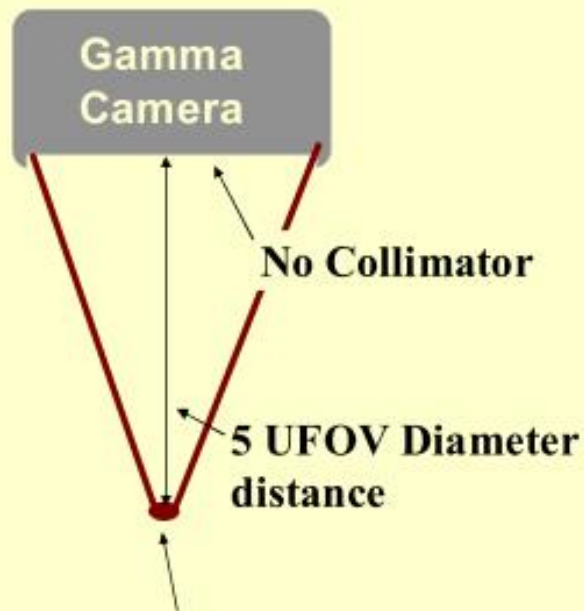


Fig. 18-14. Demonstration of effects of improved resolution on contrast and detectability of small objects. Improved spatial resolution results in improved contrast, lower right, providing improved visibility in spite of fewer counts in comparison to the other images. Decreased sensitivity of “high-resolution” collimators ultimately sets practical limits for “high-resolution imaging” in nuclear medicine. Reproduced with permission from Muehllehner G: Effect of resolution improvement on required count density in ECT imaging: a computer simulation. *Phys Med Biol* 30 (2):163–173, 1985

Measuring Intrinsic Uniformity



Point Source
400-800 uCi

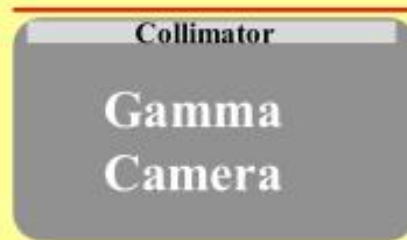


Statistical Variation:

- 3 Mcts. $\sim 1600 \text{ ct/cm}^2 (\pm 2.5\%)$
- 15 Mcts. $\sim 4800 \text{ ct/cm}^2 (\pm 1.4\%)$

Measuring Extrinsic Uniformity

Planar Source
10-15 mCi of
 ^{57}Co or $^{99\text{m}}\text{Tc}$



A circular image showing the edge packing of a planar source. The image is dark with a lighter, textured circular area in the center. An arrow points to the edge of this area, which is labeled "Edge Packing shielded by collimator ring."

Edge Packing
shielded by
collimator ring.

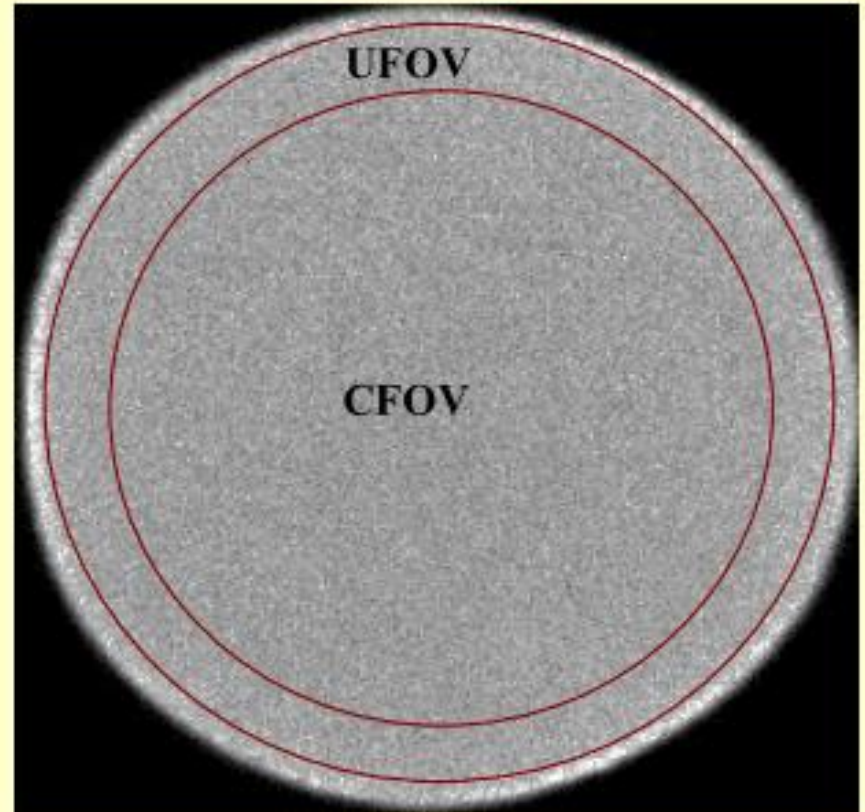
5-15 Million Counts
3-15 min.

Integral Uniformity (IU) Index

Integral Uniformity (IU)
(4000 cts/cm² with 9-pt.
smoothing in 6 mm pixels)

$$\frac{\text{Max. Pixel} - \text{Min. Pixel}}{\text{Max. Pixel} + \text{Min. Pixel}} \times 100\%$$

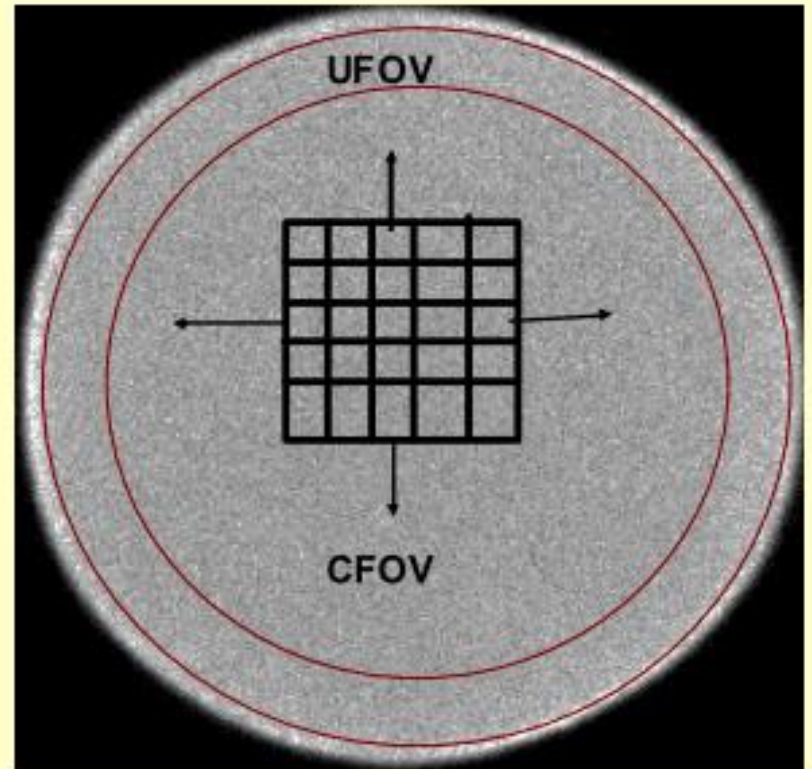
- **Range of sensitivity variations over the UFOV or CFOV**
- **IU of 2-3 % expected**



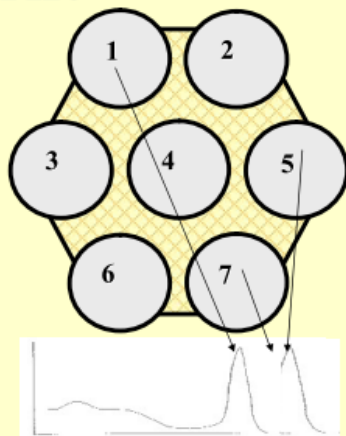
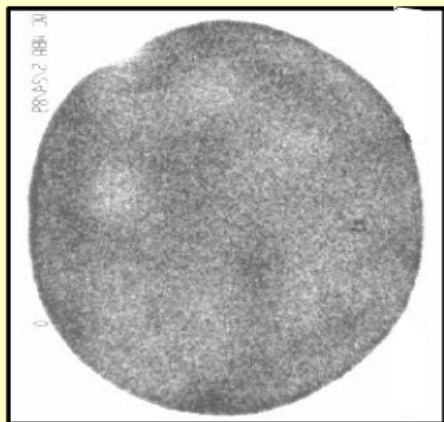
Differential Uniformity Index

Differential Uniformity (DU)

- **Maximum rate of change in sensitivity across the UFOV or CFOV**
- **DU of 1.5 – 2.0% expected.**

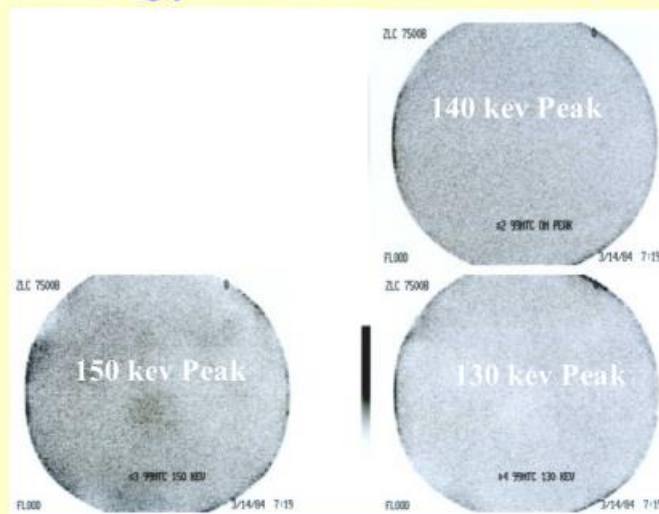


Non-Uniformity from PMT Drift

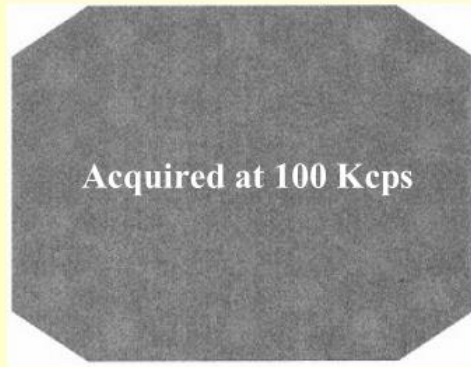


PMT voltage drift causes peak shift and difference in sensitivity.

Uniformity Dependent on Energy Window Centering

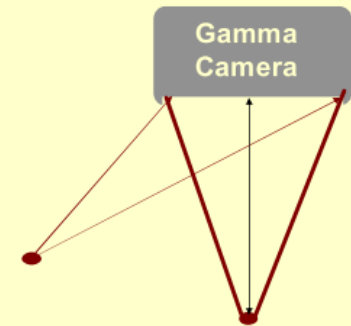
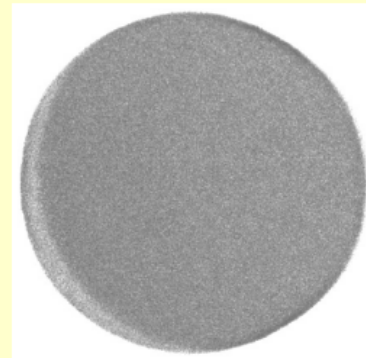


Non-Uniformity at High Count Rates



High count rates also leads to loss of resolution and linearity

Non-Uniformity From a Second Source



A second ^{99m}Tc source in the room or in the hot lab next door.
Susceptible artifact when acquiring intrinsic floods.

Non-Uniformity from Cracked/Broken Crystal

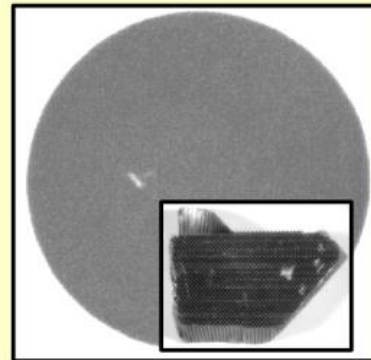
Crystal may cracked:

- from mechanical shock during collimator exchange.
- by thermal shock where the crystal temperature changes by more than 10 deg./hour.

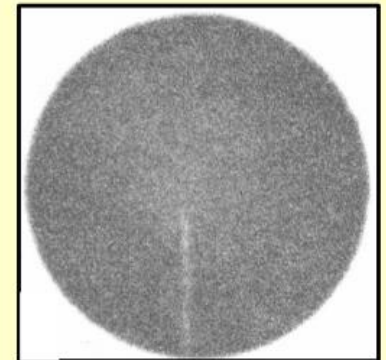


Non-Uniformity from Collimator Damage

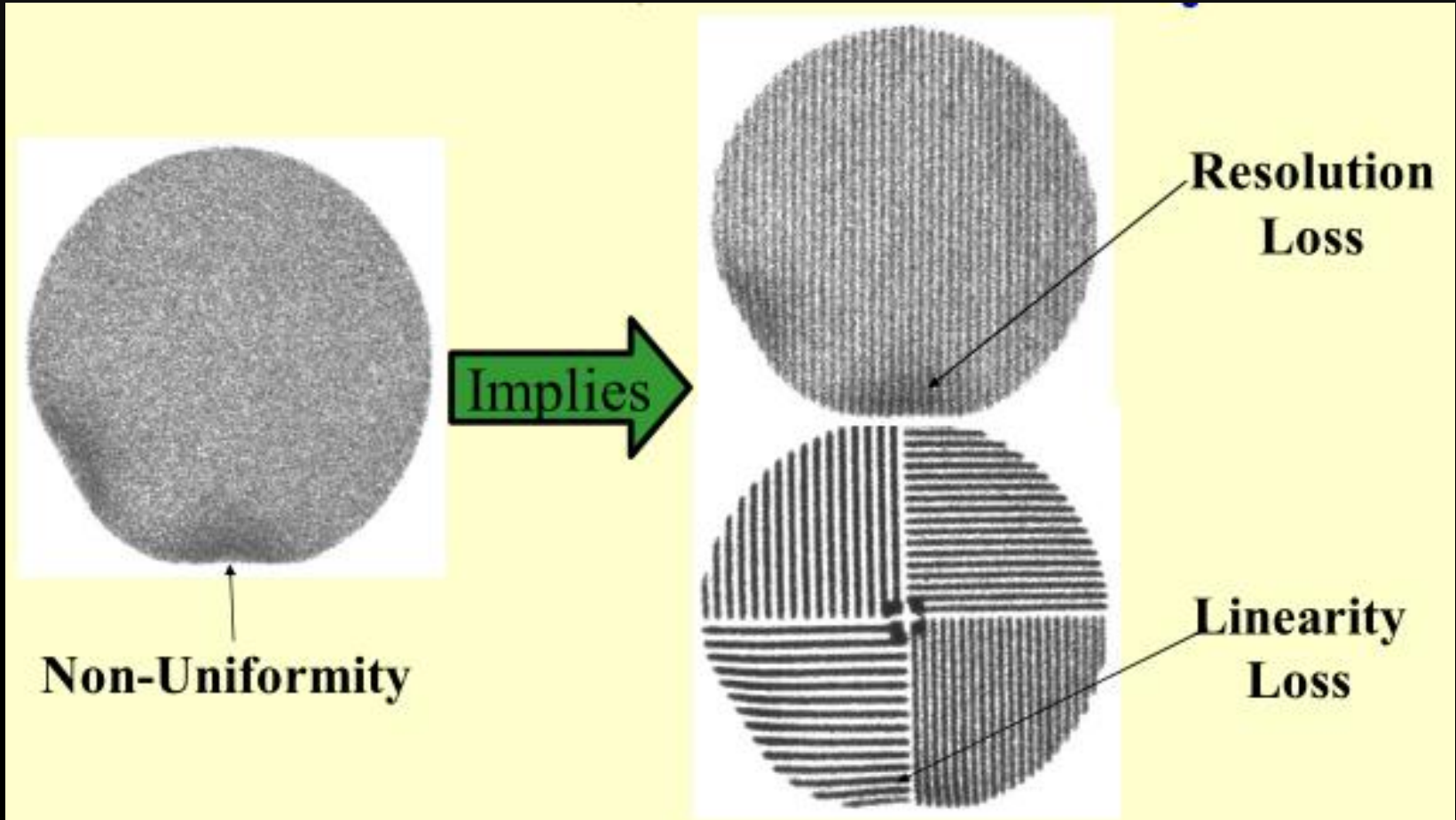
Crushed Lead Septa



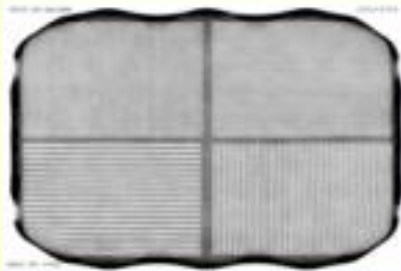
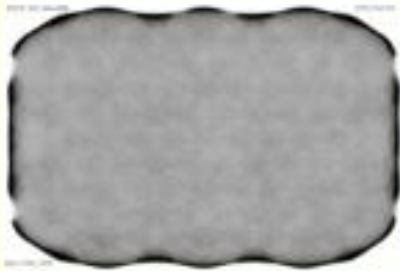
Lead Foil Separation



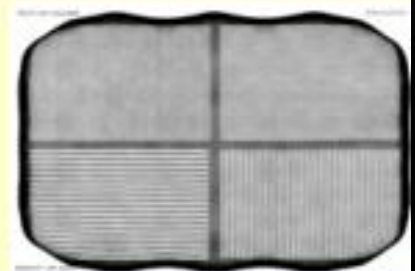
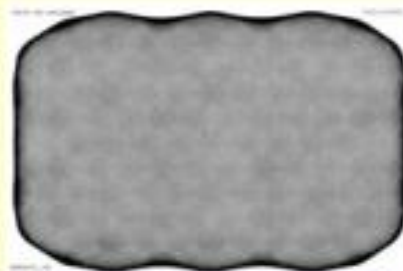
Inter-Relationship of Uniformity, Resolution, and Linearity



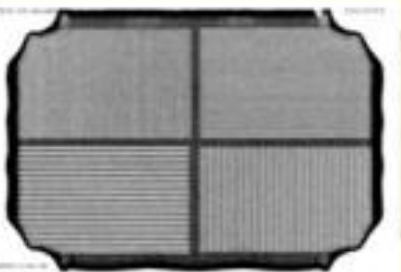
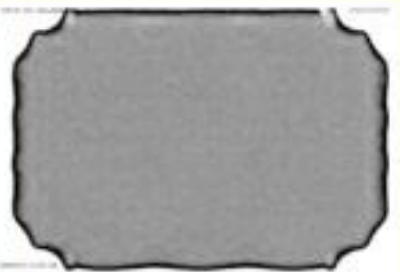
Sequential Improvement in Image Quality with added Corrections



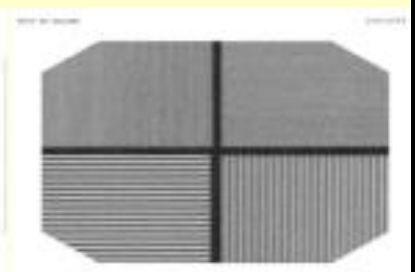
No corrections



First - Energy Correction

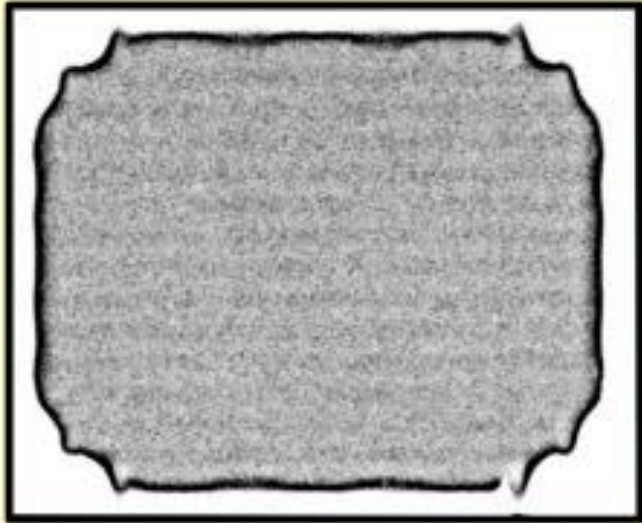


Second - Linearity Correction

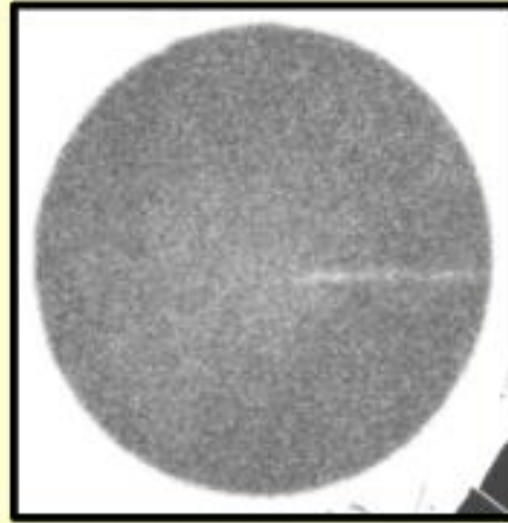


Third - Uniformity Correction

Uniformity Correction – May Mask Underlying Problems!

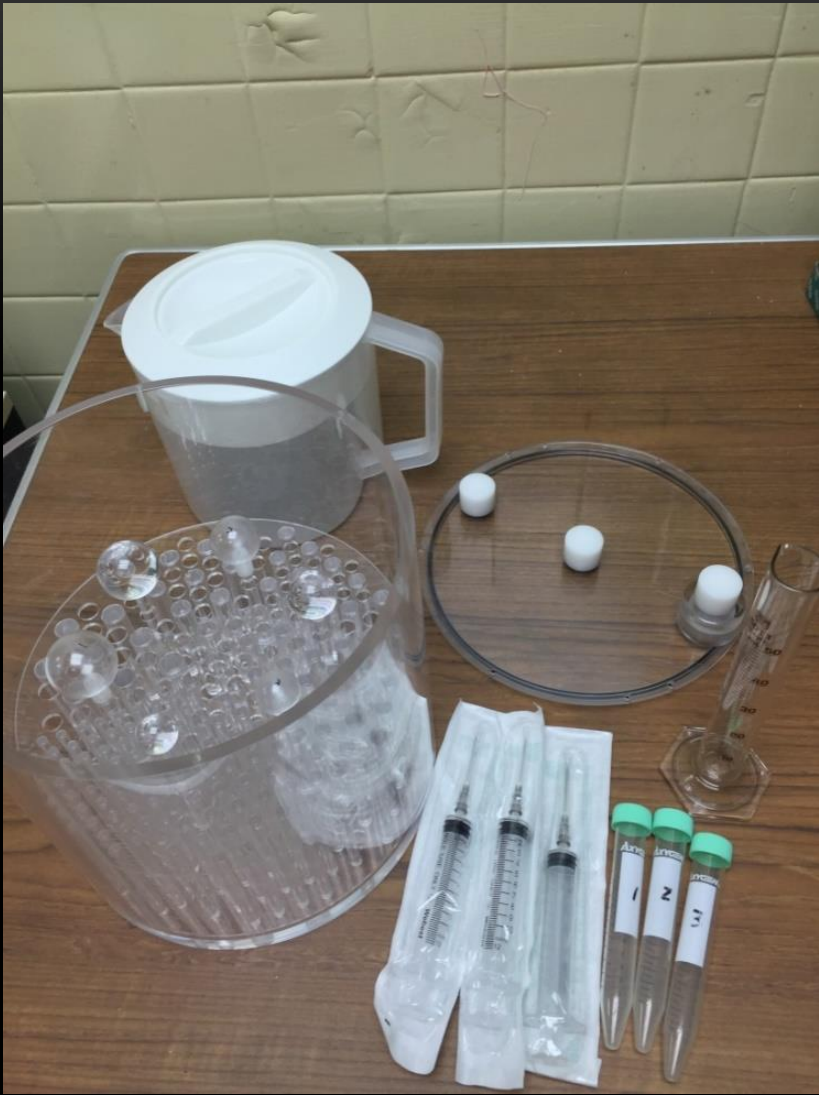


**Detector with intrinsic
linearity problems**



**Damaged collimator
with crushed lead septa**

假體灌製



Hollow Sphere Sets (6)TM

Hollow Sphere Set (6)TM

Model ECT/HS/SET6

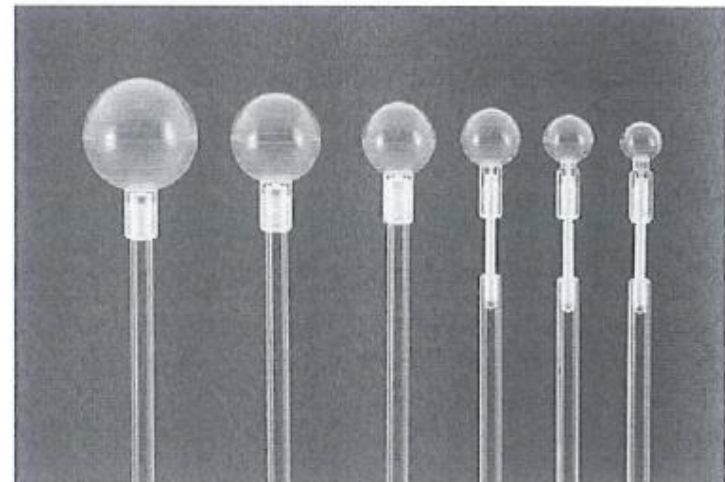
Main Applications:

- Designed for use in all circular and elliptical ECT cylinders
- Simulates hot or cold spherical “lesions”
- Quantitative evaluation of spatial resolution/object size, attenuation and scatter effects
- Evaluation of quantitative ECT reconstruction methods
- Research

Specifications:

Outer diameter: ~ 11.89 mm, ~ 14.43 mm, ~ 17.69 mm,
~ 21.79 mm, ~ 26.82 mm, ~ 33.27 mm

Volume of Spheres: ~ 0.5 mL, ~ 1.0 mL, ~ 2.0 mL,
~ 4.0 mL, ~ 8.0 mL, and ~16.0 mL

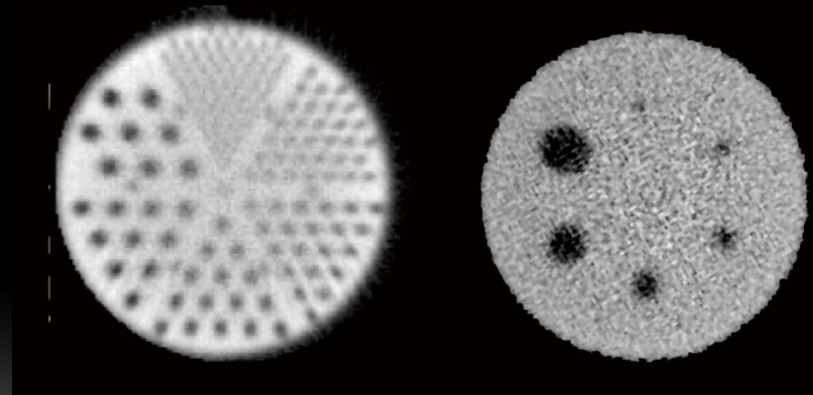
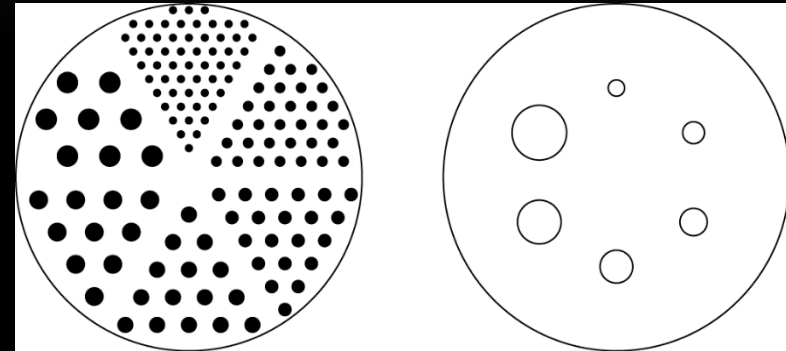


Hollow Sphere Set (6)TM

HOLLOW SPHERE OUTER DIAMETERS (OD) AND VOLUMES (APPROX.)

OD (mm)	ID (mm)	OD (cm)	OD (inches)	Measured volume (mL)
11.89	9.89	1.2	.468	0.5 mL 0.46
14.43	12.43	1.4	.568	1.0 mL 0.8 ml
17.69	15.43	1.8	.696	2.0 mL 1.8 ml
21.79	19.79	2.2	.858	4.0 mL 3.8 ml
26.82	24.82	2.7	1.056	8.0 mL 7.8 ml
33.27	31.27	3.3	1.310	16.0 mL 15.8 ml

FLANGELESS DELUXE JASZCZAK PHANTOM™ MODEL ECT/FL-DLX/P



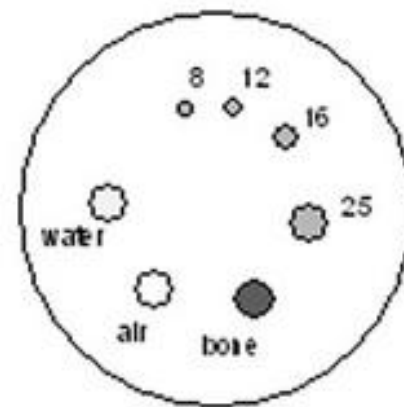
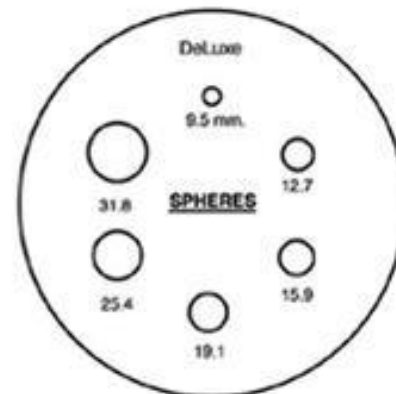
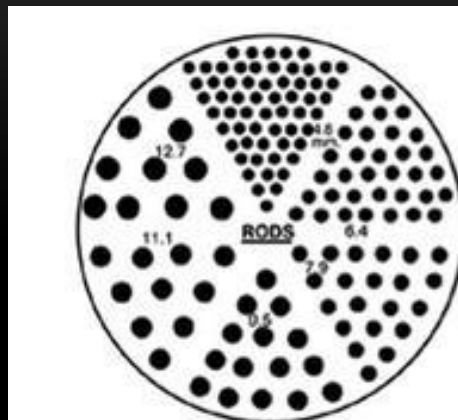
Specifications of Insert and Spheres:

Rod diameters: 4.8, 6.4, 7.9, 9.5, 11.1, and 12.7 mm

Height of rods: 8.8 cm

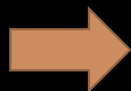
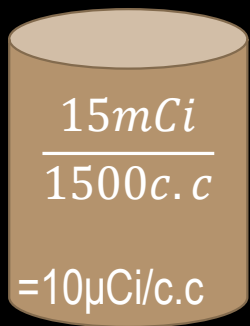
Solid sphere diameters: 9.5, 12.7, 15.9, 19.1, 25.4 and 31.8 mm

Flangeless Deluxe PET and SPECT Phantoms

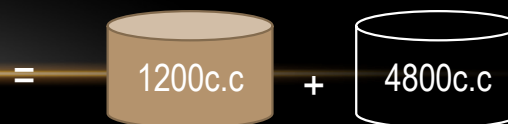


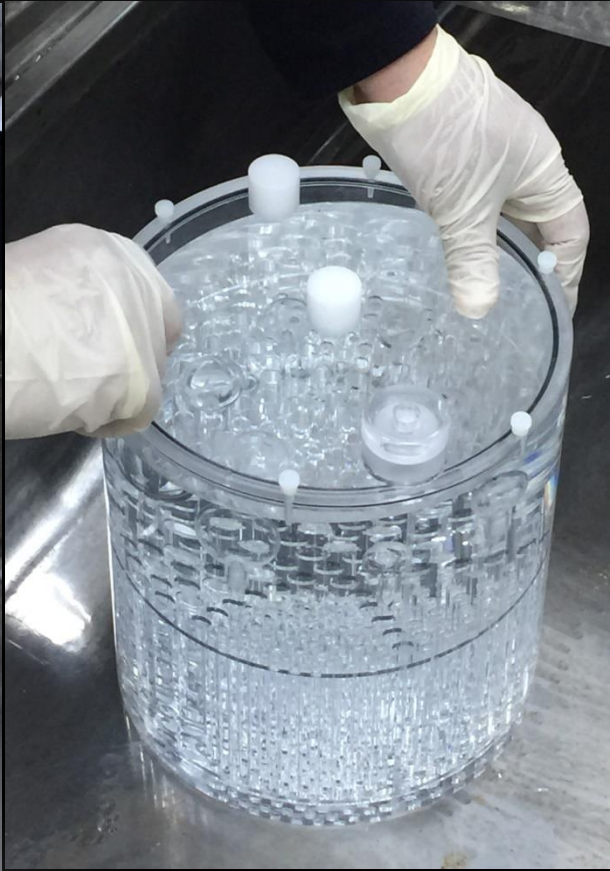
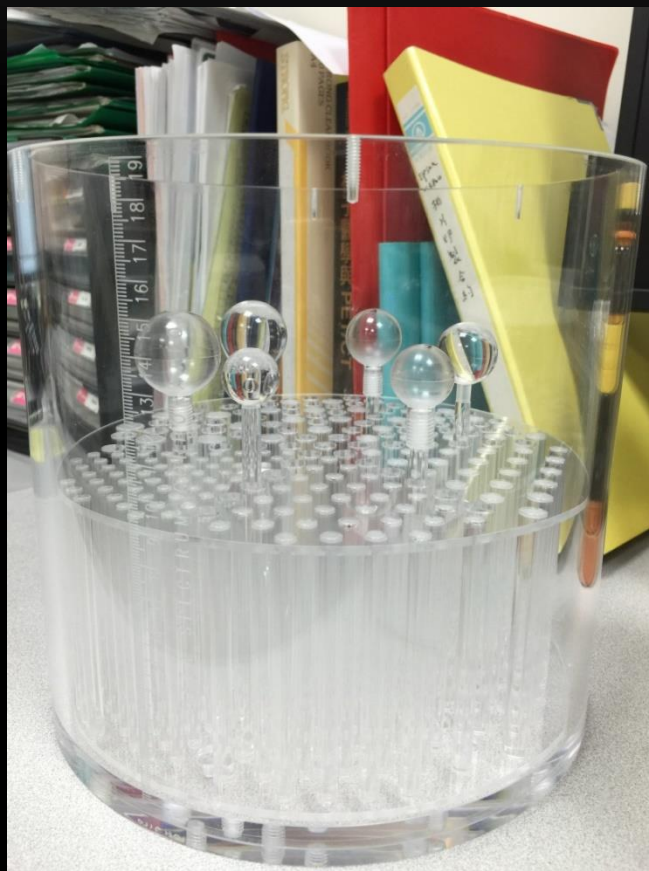
Step1

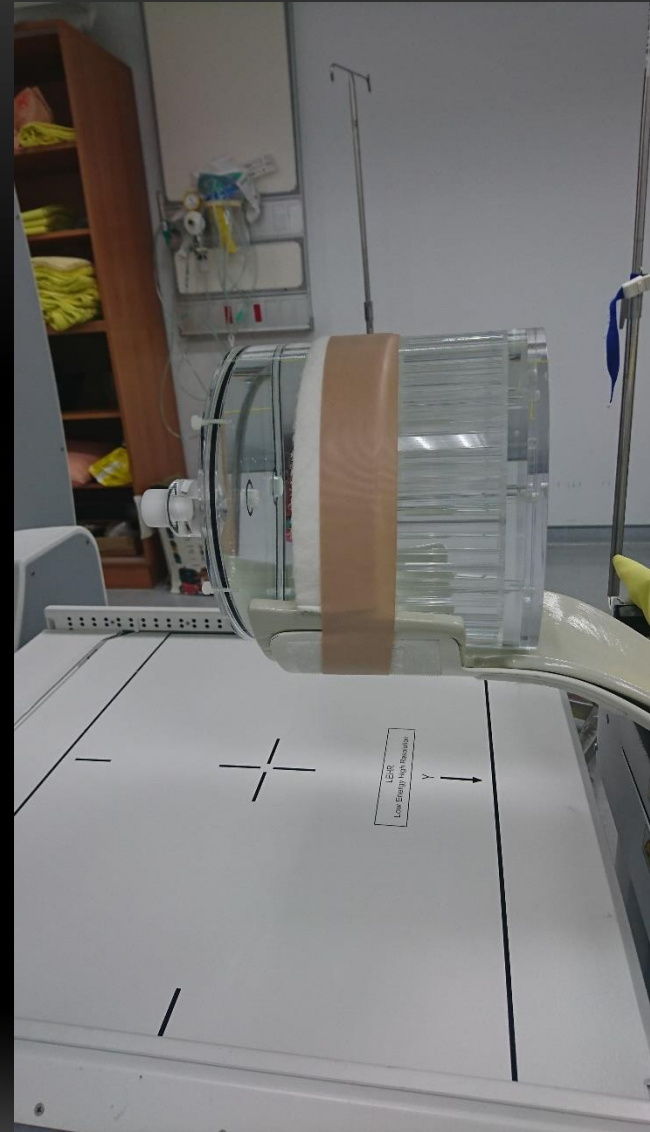
Tc 15mCi

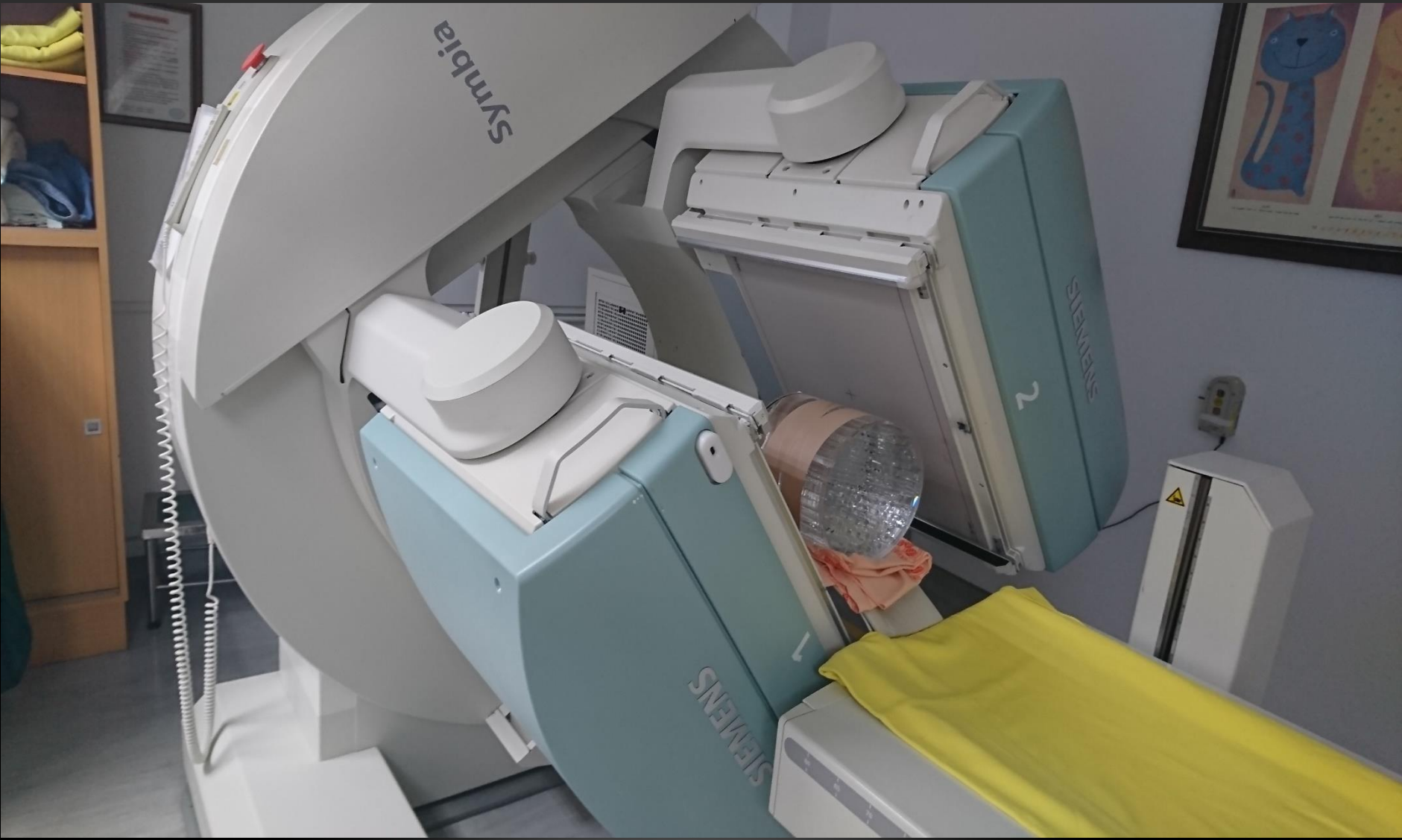


Step2









造影參數設定

Series: TRODAT-1 Brain

Summary | Series Information | Camera Parameters | Stop Conditions

Name	Description
Patient Name	Phantom Fan Beam
Patient ID	20170328
Study Name	
Series Name	TRODAT-1 Brain
Series	TRODAT-1 Brain
Technologist	
Reading Physician	
Referring Physician	
Organ	Cerebral
Isotope 1	99m Technetium, 20.00 mCi, None
Matrix Size	128 X 128
Zoom	1.00
Camera Preset	Tc99m-NMG
Detectors	Both Detectors
Orientation	Head In
Patient Position	Supine
Rotation Direction:	CW
Starting Angle:	0
Degrees of Rotation:	360
Patient State	
Number of Views:	120
Time per View:	20 sec
Detector Configuration:	180
Orbit	Circular
Mode:	Step and Shoot
Attenuation Correction	Off

99m Technetium

KCounts: 218
Remaining: 00:43:41
View: 5 of 120

99m Technetium

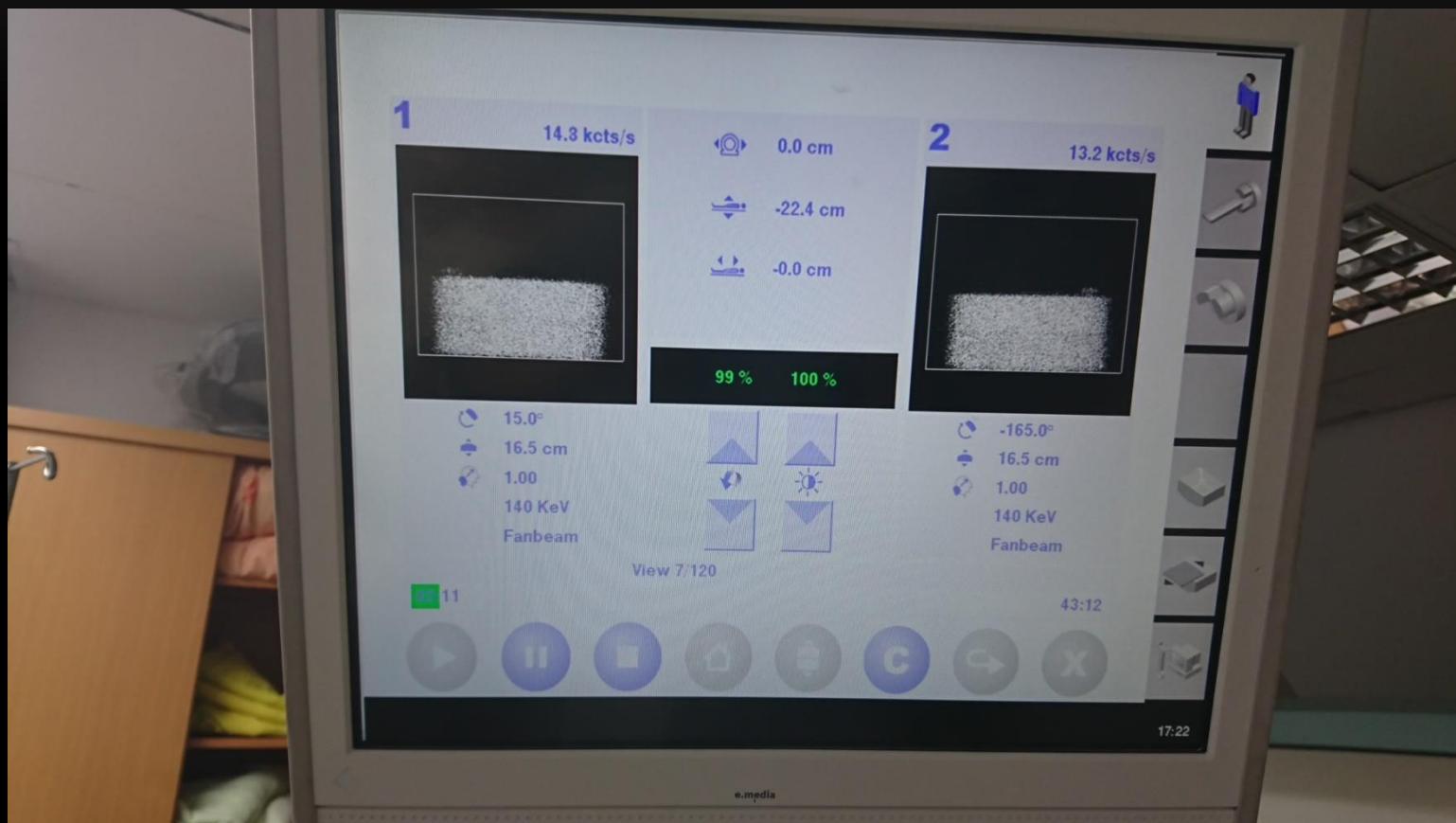
KCounts: 195
Elapsed: 00:00:14
Frames: 8 of 240 (3%)

Camera Parameters

Supine
128 X 128
1.0
Tc99m-NMG
Both Detectors

Prepare Acquisition

Complete Suspend Setup



1

13.7 kcts/s



0.0 cm

-22.4 cm

-0.0 cm

99 % 100 %

-126.0°
 16.5 cm
 1.00
 140 KeV
 Fanbeam



2

14.0 kcts/s



54.0°
 16.5 cm
 1.00
 140 KeV
 Fanbeam

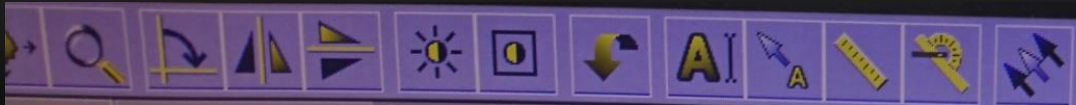
View 79/120

29:04

15:37



17:49



analyzer Display/Analysis

Presets

Existing Preset: [Dropdown]

Preset Name: [Text Field]

Save Preset [Button]

Detector Status

Detector 1
 Detector 2

Dead Time (%)	Peak Status	1	2	3	4	5	6	7	8
3.75	PEAKED	-0.06							
3.50	PEAKED	-0.29							

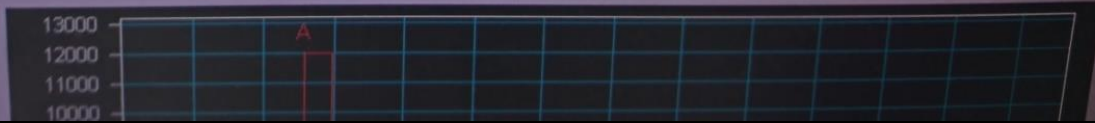
Pause Between Peaks

Window Number	Center (keV)	Width (%)	Shift (%)	Type	Parent
A1	140	15	0	Photopeak	

Window Center (keV): [Text Field] Window Width (%): [Text Field] Window Shift (%): [Text Field]

Window Group A: 99m Technetium [Dropdown]

Window Group B: [Dropdown]





Patient Name: Phantom LEHR

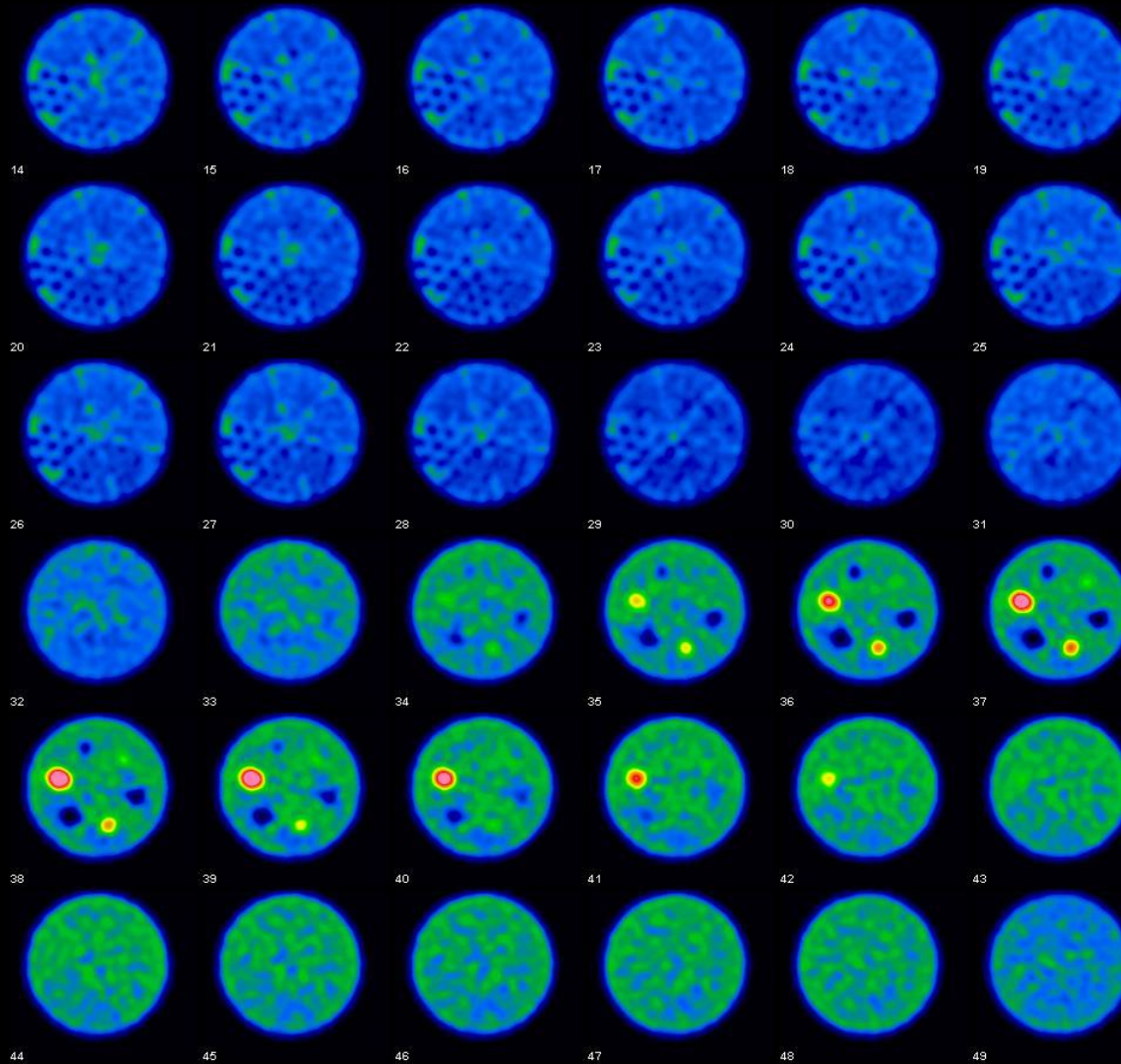
Patient Id: 20170328++1+

VGH TPE

Study Name: TRODAT_SPECT-CT

Date & Time: 3/28/2017

Manufacturer Model: Tandem_Discovery_670



Feet to Head

Transversal

LEHR no Filter (FBP)

LEHR no Filter (OSEM)



Patient Name: Phantom LEHR

Patient Id: 20170328++1+

VGH TPE



Study Name: TRODAT_SPECT-CT

Date & Time: 3/28/2017

Manufacturer Model: Tandem_Discovery_670

Patient Name: Phantom LEHR

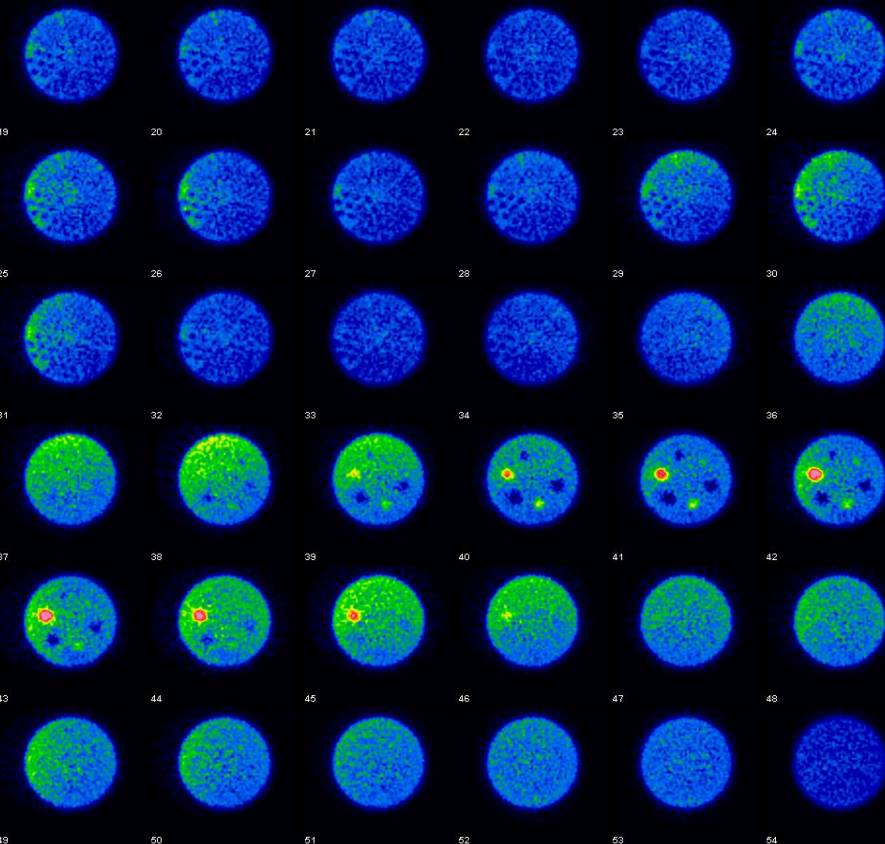
Patient Id: 20170328++1+

VGH TPE

Study Name: TRODAT_SPECT-CT

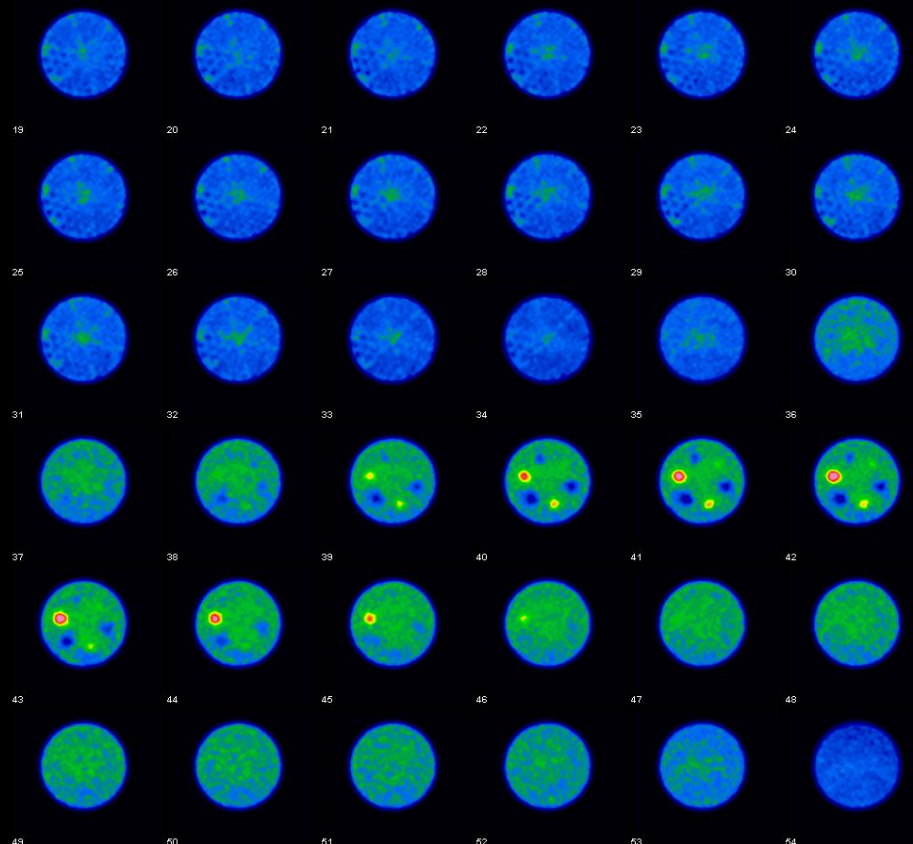
Date & Time: 3/28/2017

Manufacturer Model: Tandem_Discovery_670



Feet to Head

Transversal

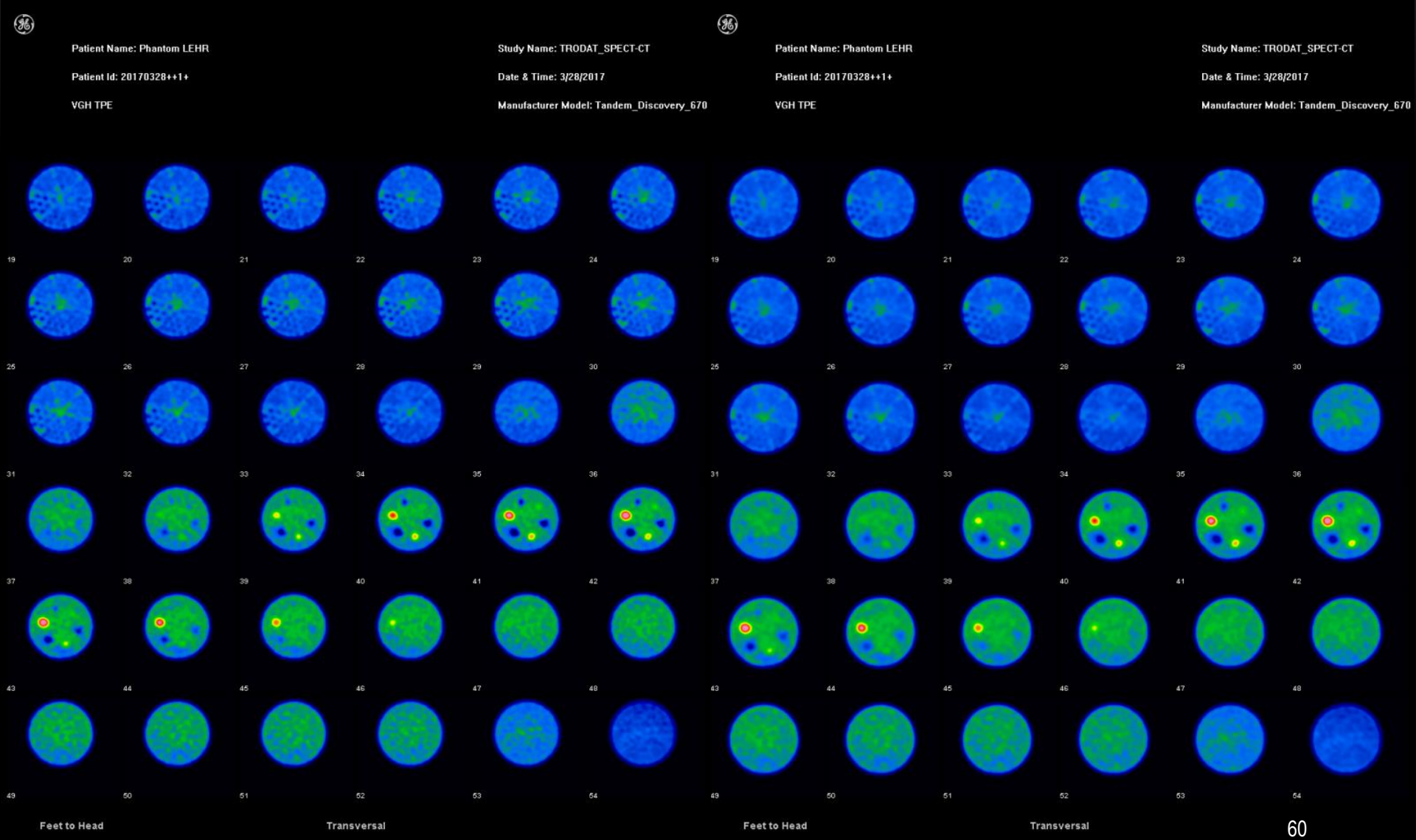


Feet to Head

Transversal

LEHR BW 0.46 10 (FBP)

LEHR BW 0.46 10 (OSEM)



24 HR LEHR no Filter (FBP)

24 HR LEHR no Filter (OSEM)



Patient Name: Phantom LEHR-24hr

Patient Id: 20170329

VGH TPE

Study Name: TRODAT_SPECT-CT

Date & Time: 3/29/2017

Manufacturer Model: Tandem_Discovery_6



Patient Name: Phantom LEHR-24hr

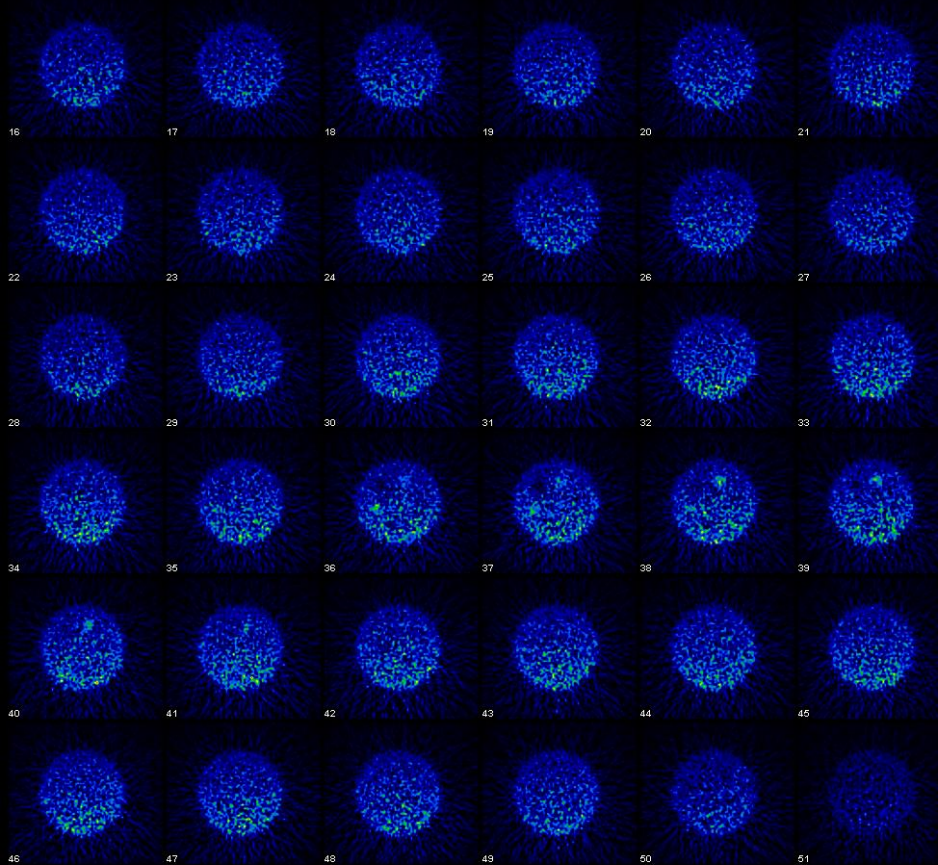
Patient Id: 20170329

VGH TPE

Study Name: TRODAT_SPECT-CT

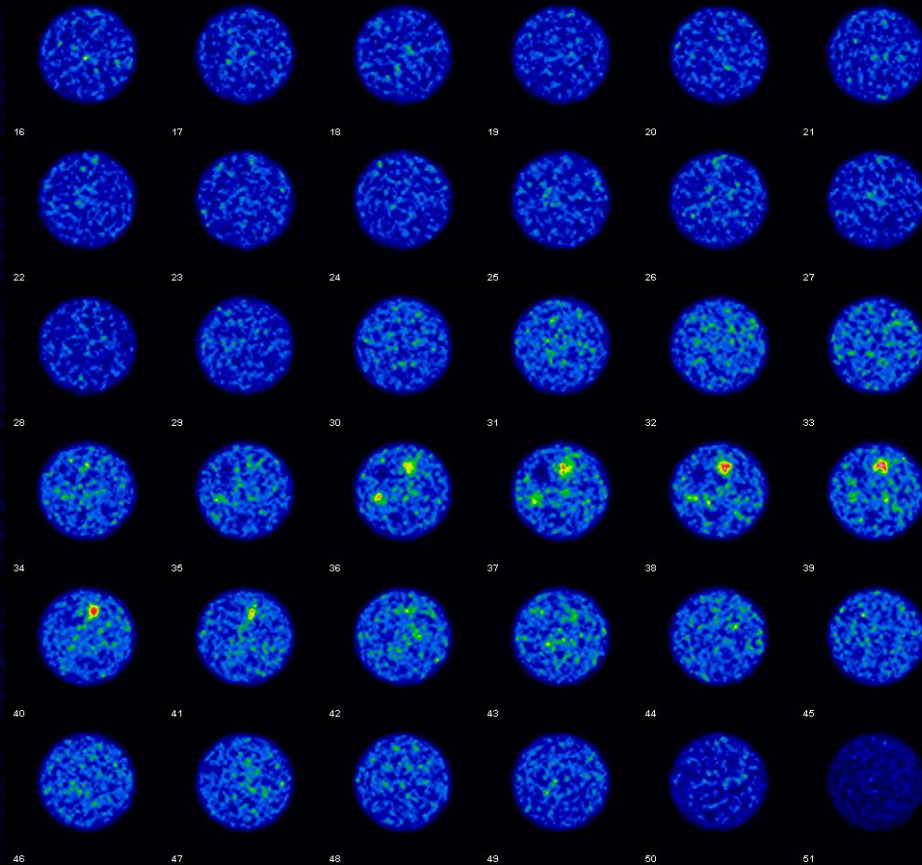
Date & Time: 3/29/2017

Manufacturer Model: Tandem_Discovery_670



Feet to Head

Transversal



Feet to Head

Transversal

24 hr LEHR BW 0.46 10 (FBP)

24 hr LEHR BW 0.46 10 (OSEM)



Patient Name: Phantom LEHR-24hr

Patient Id: 20170329

VGH TPE

Study Name: TRODAT_SPECT-CT

Date & Time: 3/29/2017

Manufacturer Model: Tandem_Discovery



Patient Name: Phantom LEHR-24hr

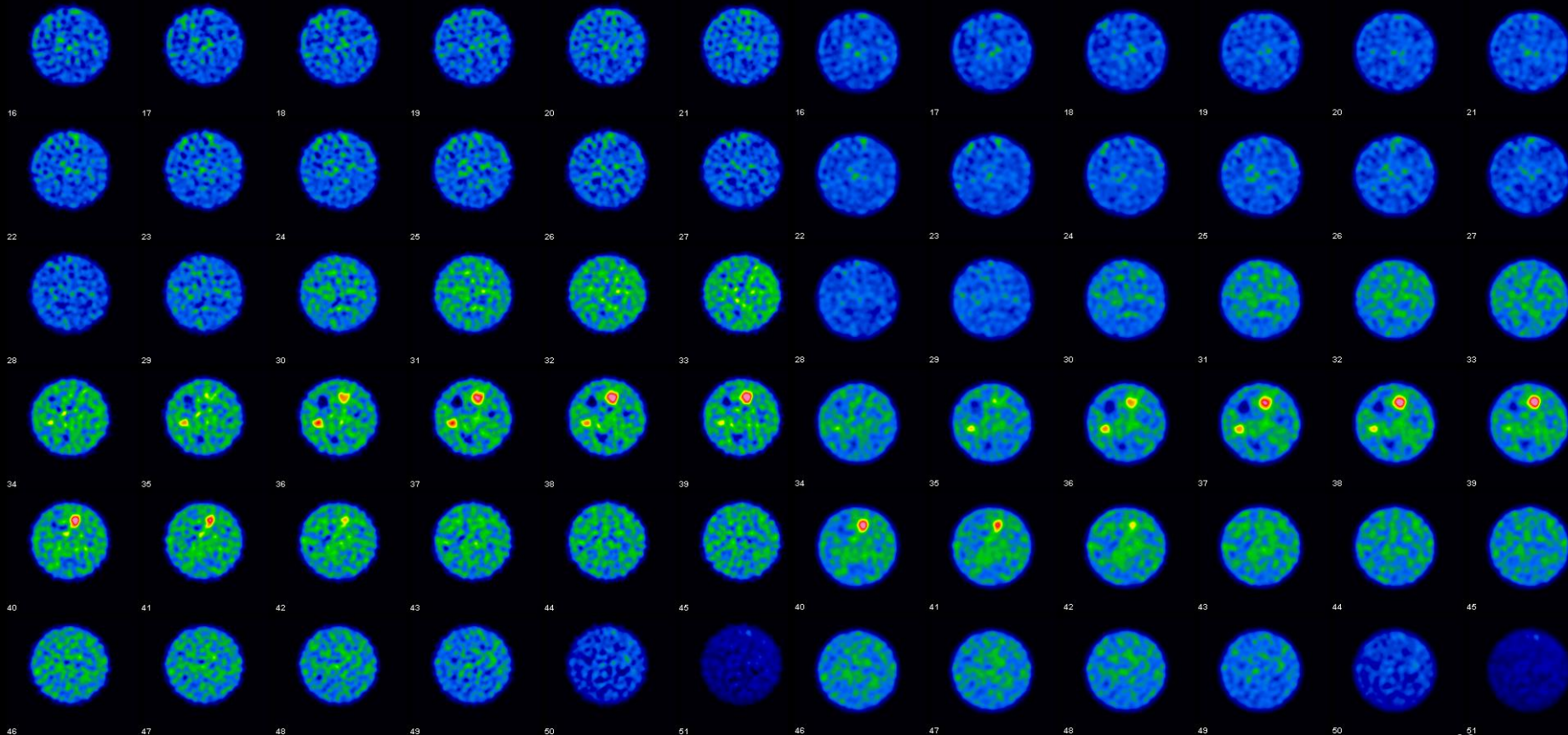
Patient Id: 20170329

VGH TPE

Study Name: TRODAT_SPECT-CT

Date & Time: 3/29/2017

Manufacturer Model: Tandem_Discovery_670



Feet to Head

Transversal

Feet to Head

Transversal

Fan BW 0.46 10 (FBP)

Fan BW 0.46 10 (OSEM)



Patient Name: Phantom Fan Beam

Patient Id: 20170328

VGH-TPE

Study Name: 1

Date & Time: 3/28/2017

Manufacturer Model: IP2



Patient Name: Phantom Fan Beam

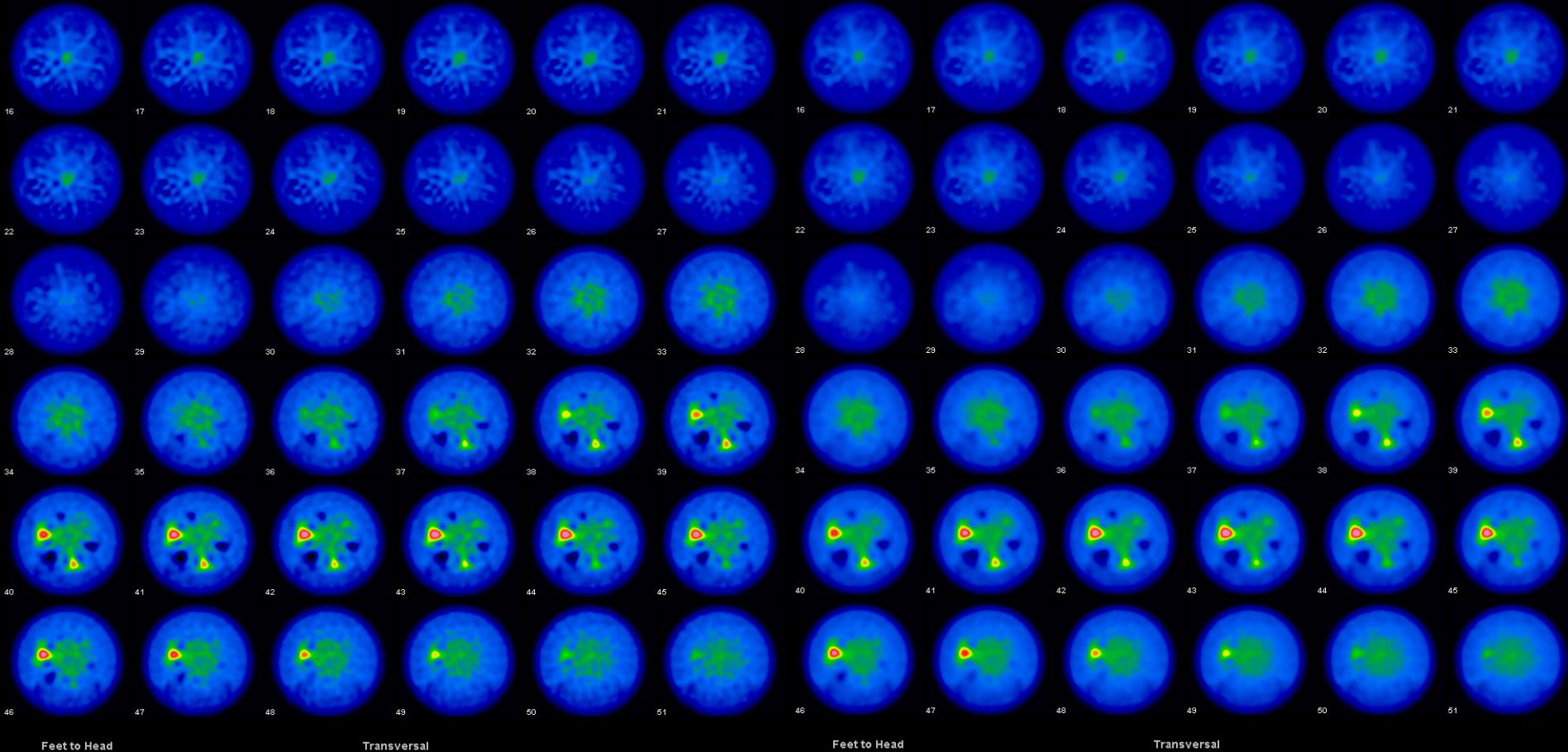
Patient Id: 20170328

VGH-TPE

Study Name: 1

Date & Time: 3/28/2017

Manufacturer Model: IP2



Feet to Head

Transversal

Feet to Head

Transversal

核子醫學科 閃爍攝影機及影像品管程序 調查表

醫院名稱:

Gamma Camera 型號:

裝設時間: 年

偵測頭: single dual

影像品管:

品管項目	每日	每週	每月	每季	每半年	每年	NC
Flood Uniformity(掛 collimator)							
Flood Uniformity(不掛 collimator)							
Spatial Resolution(Bar Phantom)							
Spatial Energy resolution							
Count rate performance							
Sensitivity map							
Linearity							
multiple window resolution							
Center of Rotation							
SPECT reconstruction							
System Alignmant							
System Volume sensivity							
Whole body system spatial resolution							

品管射源: point source (mCi) Flood Source (Co57 mCi)

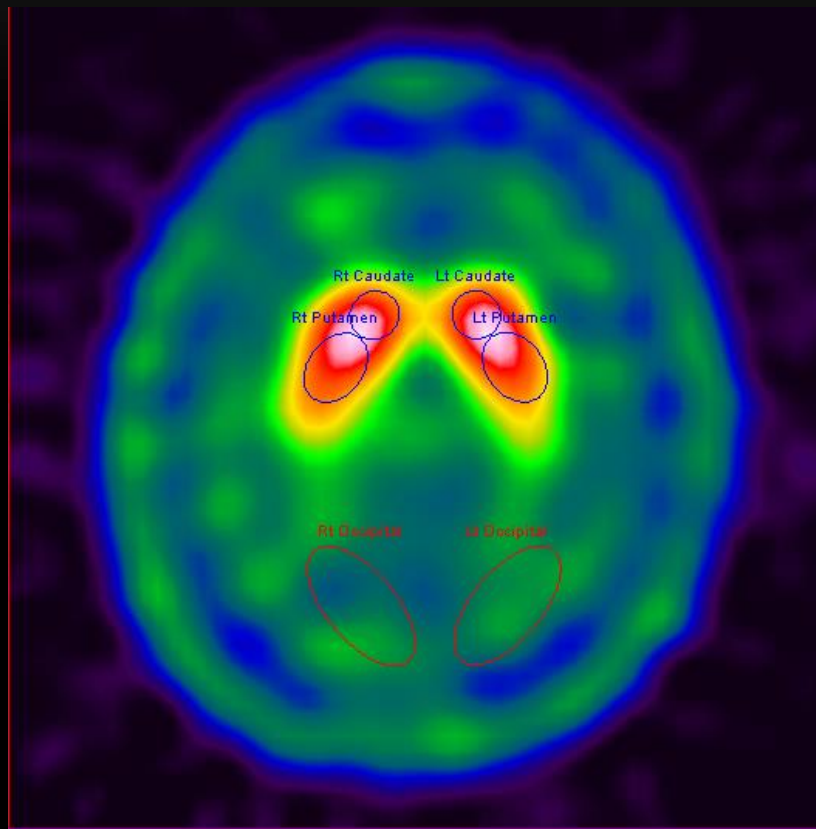
Flood Uniformity 平均值為 (Head 1 %, Head 2 %)

每日 QC 所耗時間: 分鐘

PS: 請以 Gamma Camera 為單位填寫

感謝您的支持!!

SEMI-QUANTITATIVE ANALYSIS



- Specific uptake ratio (SUR)

$$SUR = \frac{\text{target} - \text{background}}{\text{background}}$$

*target : striatum, caudate or putamen

*background : occipital cortex, frontal cortex
or cerebellum

* unit : counts/voxel

- Asymmetry

$$\text{Asymmetry} = \frac{|SUR_{\text{right striatum}} - SUR_{\text{left striatum}}| \times 2}{SUR_{\text{right striatum}} + SUR_{\text{left striatum}}} \times 100\%$$

IMAGE QUALITY

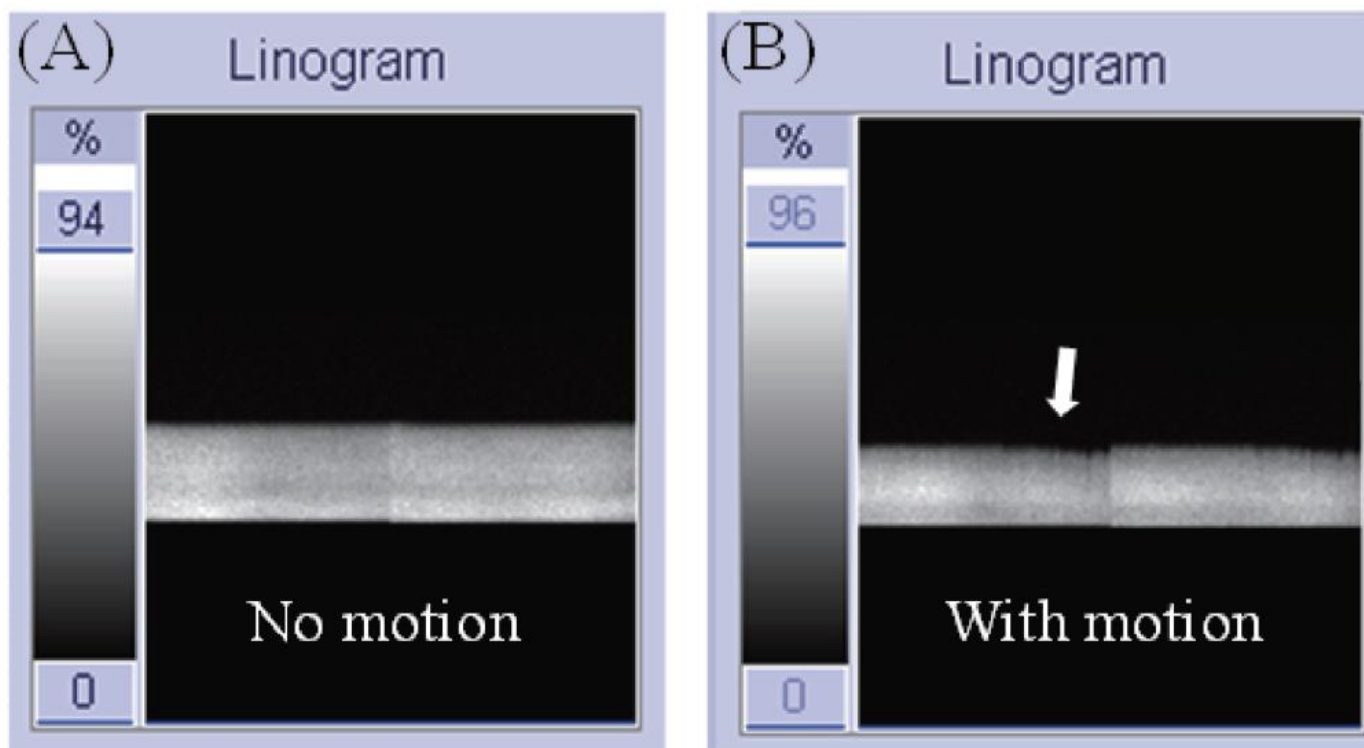
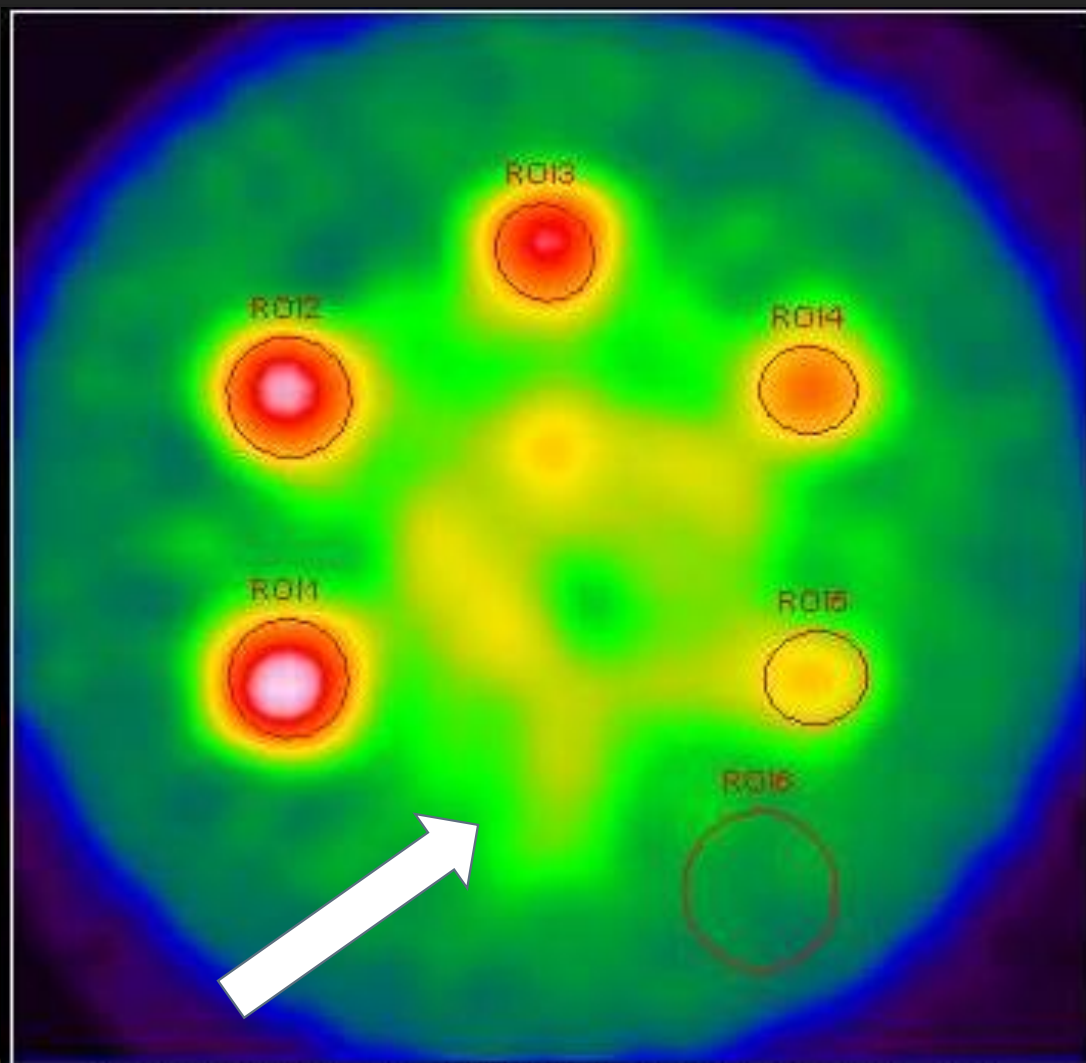
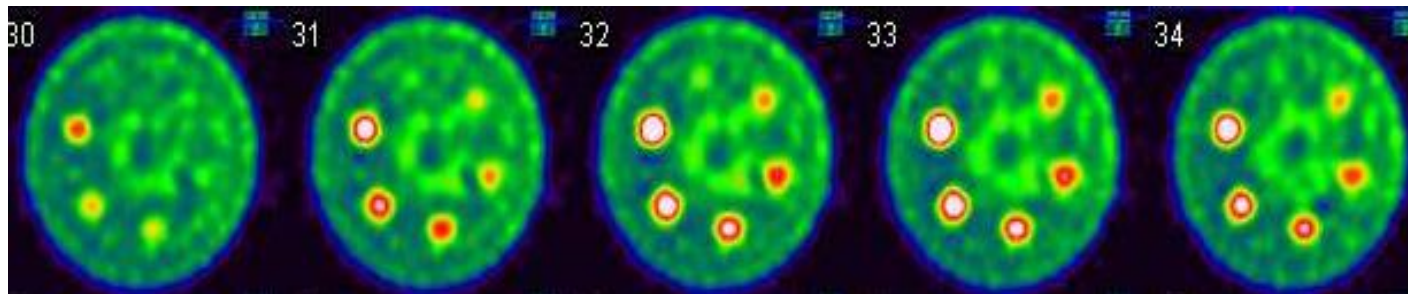


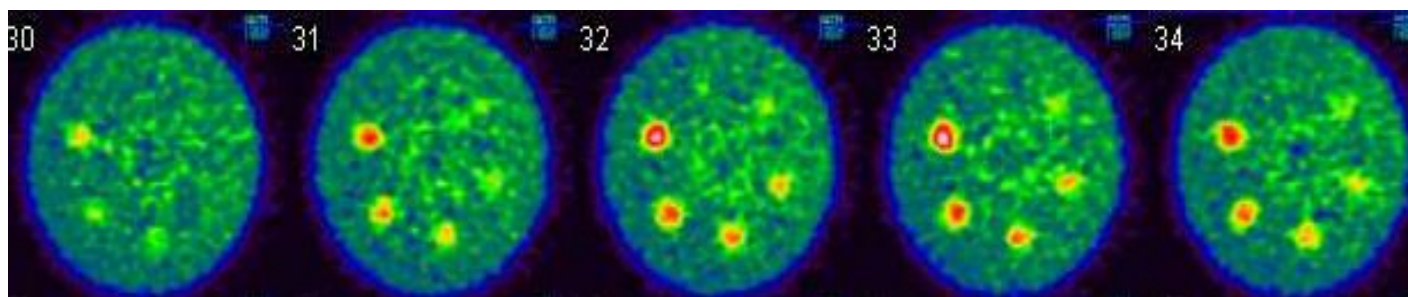
Figure 2. Motion can be observed by linogram in SPECT scans. (A) is without motion. (B) shows some streak on linogram with motion (arrow).



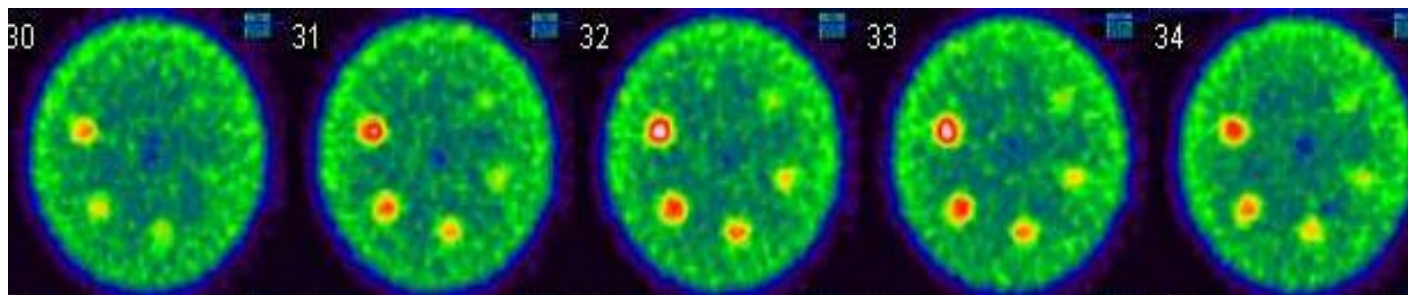
均勻水假體發現有環狀活性假影



(A) Metz filter

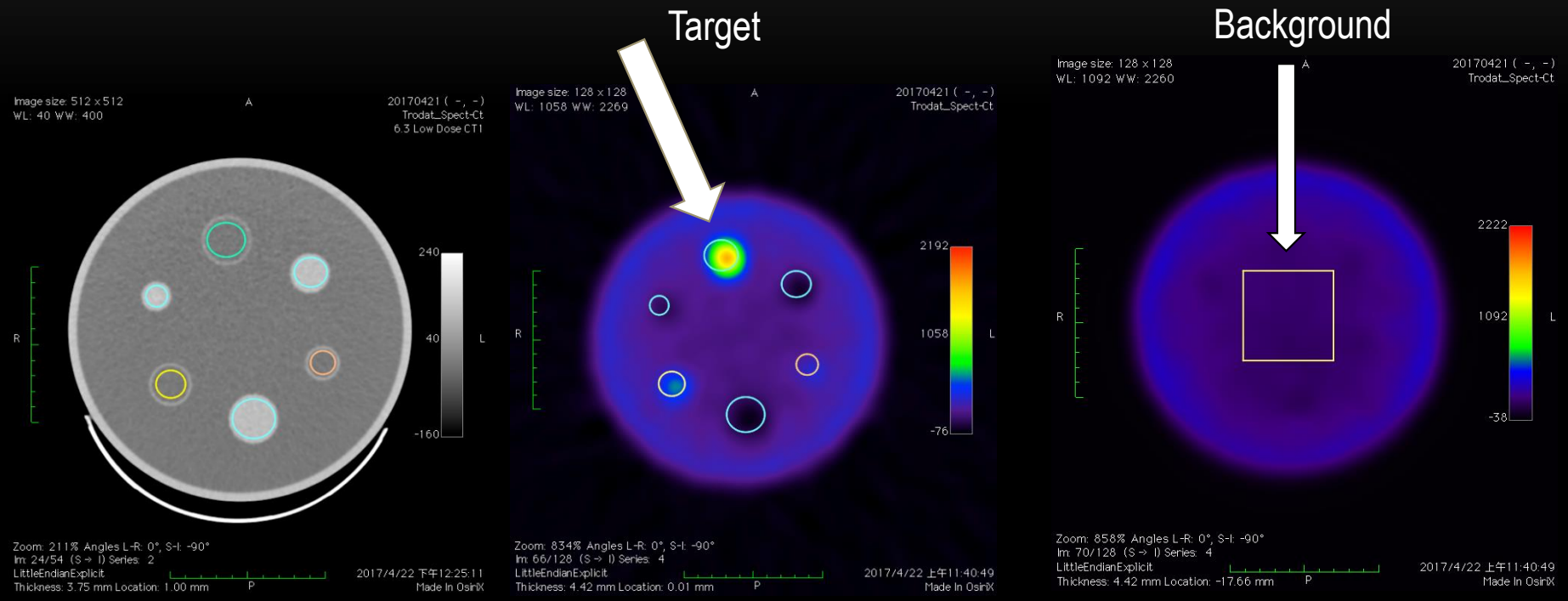


(B) Butterworth filter



(C) Non filter

最後將獲得的SPECT影像，圈選ROI的位置，並與原本預計調配的活性比值，互相比較分析



結論

TRODAT影像品質受到很多影響，再掃描前建議如下

1. 儀器品保要確實，尤其旋轉中心(COR)等
2. 影像重建法影像TRODAT影像很大，不同重建法或是使用不同的濾波器都會造影影像品質不同，有些條件甚至造成放射熱區或是球體實心空白區影像變形扭曲，故建議可以利用假體影像找出最適合該醫院醫師讀片之條件為主。
3. TRODAT影像受限於腦部吸收的數值偏低，無論選擇平行孔準直儀、扇形準直儀，都建議需要固定造影參數，影像矩陣大小、選轉360度收集影像、Zoom的大小等等都需要小心注意。